PHYSICAL REVIEW D **88,** 033004 (2013)

Effective gauge-Higgs operators analysis of new physics associated with the Higgs boson

We-Fu Chang,* Wei-Ping Pan,† and Fanrong Xu‡

Department of Physics, National Tsing Hua University, HsinChu 300, Taiwan

(Received 4 April 2013; published 14 August 2013)

We study the new physics related to the recently discovered 125 GeV Higgs by employing an important subset of the standard model (SM) gauge-invariant dimension-6 operators constructed by the SM Higgs and gauge fields. Explicitly, we perform a model-independent study on the production and decays of the Higgs, the electric dipole moments (EDMs) of the neutron and the electron, and we take into account the anomalous magnetic dipole moments of the muon and electron as well. We find that, even if all Higgs decay channels agree with the SM predictions, the SM theoretical uncertainties provide a lot of room to host new phyiscs associated with the 125 GeV boson. A linear relation is revealed in our numerical study that $\mu_{ZZ} \simeq \mu_{WW}$ and $0.6 \lesssim \mu_{ZZ,WW} \lesssim 1.4$ at 95% C.L. with or without the EDM constraints. The neutron and electron EDMs severely constrain the relevant Wilson coefficients. Therefore the CP-violating components in the $h \to WW$, ZZ channels are too small, $\sim\mathcal{O}(10^{-5})$, to be detected at the LHC. However, we point out that, even though the parity of the 125 GeV boson has been largely determined to be even in the $h \to ZZ$ channel, one should pay special attention to the potentially large CP violation in the $h \to \gamma\gamma$ and $h \to \gamma Z$ channels. This should be seriously checked in the future spin correlation experiments.

DOI: 10.1103/PhysRevD.88.033004 PACS numbers: 14.80.Bn, 11.30.Er, 12.60.Fr

I. INTRODUCTION

The high-energy physics community has been excited about the recent finding of a standard model (SM)-like Higgs boson h, the final piece of the SM we had long craved, at the mass around 125 GeV at the LHC [1,2]. So far, except the Higgs diphoton decay, which is $\sim 1\sigma$ higher than its SM prediction, all other Higgs decay modes agree with the SM predictions within the experimental accuracies [3–20]. The diphoton excess could be just the statistical fluctuation or due to some unknown systematic error, or it indicates the existence of new physics (NP), especially those connecting the Higgs and gauge sectors. Since last year, there has been much discussion and speculation about the diphoton excess; see, for example, Ref. [21]. Whether the diphoton excess is due to new physics or not will be settled by more experimental efforts in the coming years. Although the statistics is still weak, the current Higgs decay data have already set some limits to the NP associated with the Higgs boson. On the other hand, we should also bear in mind that the uncertainty of the SM theoretical prediction for the Higgs productions range from $\sim$2% for the vector boson fusion (VBF) to $\sim$15% for the gluon-gluon fusion (GF) [22], the dominate Higgs production mechanism at the LHC; see Table II. As for the decay branching ratios, the theoretical uncertainties range from $\sim$3% for $h \to bb$ to $\sim$12% for $h \to c\bar{c}$ [22]; see Table III. So even the experimental precision can be improved to reach the few percent level in the future; still, we will not be able to conclude the total absence of NP associated with the $\sim$125 GeV boson. The interesting question will then be the following: How much room for new physics is still allowed due to the intrinsic SM theoretical uncertainty? The main purpose of this paper is to aim for a model-independent constraint on the new physics associated with the Higgs based on the current and future data.

Meanwhile, the mass scale of exotic degrees of freedom (DOF) has been pushed to be greater than around (0.4–8) TeV in various scenarios with different assumptions [23,24]. Although a general analysis is lacking, it is now wildly believed that the cutoff scale, Λ, for physics beyond SM which begins to show up, should be much greater than the electroweak symmetry breaking scale, $v \sim 250$ GeV. Motivated by the diphoton excess and the exotic DOF(s) that is (are) heavier than the electroweak scale, it is reasonable to assume that the new physics effects can be captured and described by the dimension-6 (dim-6) gauge-Higgs operators. We assume that the NP decouples at $\Lambda \gg v$ where the SM electroweak symmetry is not yet broken. Below the cutoff, there are only SM DOFs, and the SM gauge symmetry is still honored by the low-energy effective theory. The information and effects of NP are encoded in the form of the effective operators and their corresponding Wilson coefficients; see Refs. [25,26] for the early general discussion. It is not new to study the Higgs physics by using the gauge-Higgs operators; see Refs. [27–31] for the previous studies along the same line and Ref. [32] for recent update including the Moriond 2013 data. However, some constraints have been overlooked by those authors. The current analysis is so far the most comprehensive one to our best knowledge. We found that those contributions that had been overlooked indeed play a significant role to constrain NP.

*wfchang@phys.nthu.edu.tw
†two.joker@gmail.com
‡frxu@phys.nthu.edu.tw

In this work we shall perform a model-independent analysis based on a subset of SM gauge-invariant dim-6 gauge-Higgs operators. The presence of these dim-6 operators modifies the gauge-Higgs couplings, leading to different Higgs decay and production at the tree-level. We should discuss the constraints on the relevant Wilson coefficients based on the LHC Higgs data and compare them to a benchmark case in which all Higgs decay channels sit at the predicted SM values and the SM theoretical uncertainties are used as the experimental errors. We shall show that indeed the parasitic NP can live comfortably within the SM theoretical uncertainties without much upsetting of the global fit.

In addition to the tree-level processes, the coefficients of CP-odd operators can be further constrained by estimating the loop-induced electric dipole moment (EDM) at low energy. The apparent drawback of using effective operators is that we do not have a sensible prediction of the quantum effects at the loop level. The dim-6 gauge-Higgs operators do not close under the renormalization group (RG) running [30]. To proceed, we consider the class of new physics in which the fermion EDM operators can be ignored at Λ[1] and the divergent part of loop integral can be removed by the counter terms. Practically, we use dimensional regularization to calculate the leading contribution of the CP-odd operator to the fermion EDM in the modified minimal subtraction ($\overline{\text{MS}}$) scheme. Similarly, just for a ballpark estimation of how the $(g-2)$ will limit the NP, without any better argument, we also assume the charged lepton $(g-2)$ is negligible at Λ. We calculate the loop-induced muon and electron $(g-2)$ by using the gauge-Higgs operators at low energy and further constrain the relevant CP-even Wilson coefficients. At the end, we will discuss a UV-complete toy model as an example for this assumption to work. But we should keep in mind that this assumption is not valid for the general case.

The paper is organized as follows. In Sec. II, we will lay out the important subset of the dim-6 gauge-Higgs operators. The needed Feynman rules for later calculation will be summarized there. The modifications to the Higgs decay and production due to these gauge-Higgs operators at the tree level will be discussed in Sec. III. The 1-loop contributions to EDM and $g-2$ will be given in Sec. IV. In Sec. V, we present the numerical results and some remarks from the global fitting. In Sec. VI, we briefly discuss how a degenerate solution can be resolved by the Higgs pair-production cross section. As an example of the UV origin of the gauge-Higgs operators and to illustrate in what condition our analysis is valid, two simple models with a scalar color octet, but in different $SU(2)$ representations, will be discussed. A brief summary will be given there as well. Finally, some technical details will be collected in the Appendix.

[1]This working assumption is also reasonable from phenomenology point of view. The current experimental limits require that the cutoff scale of these EDM operators to be greater than 10^4 TeV if the corresponding Wilson coefficients are all $\sim\mathcal{O}(1)$. Here, we further assume the relevant Wilson coefficients for fermion EDMs generated by higher loops at Λ or RG running are negligible.

II. EFFECTIVE LAGRANGIAN

As discussed in the previous section, we assume that the NP associated with the SM Higgs production and decay could be largely captured and described by a set of $SU(3)_C \times SU(2)_L \times U(1)_Y$-invariant dim-6 gauge-Higgs effective operators and their Wilson coefficients [28,33]:

$$\mathcal{L}_{\text{NP}} = \sum_i (c_i \mathcal{O}_i + \tilde{c}_i \tilde{\mathcal{O}}_i) \qquad (\text{i} = 1, 2, 12, 3). \tag{2.1}$$

The relevant effective gauge-Higgs operators are

$$\begin{aligned}
\mathcal{O}_1 &= \frac{g_1^2}{2\Lambda^2} H^\dagger H B_{\mu\nu} B^{\mu\nu}, \\
\tilde{\mathcal{O}}_1 &= \frac{g_1^2}{2\Lambda^2} H^\dagger H B_{\mu\nu} \tilde{B}^{\mu\nu}, \\
\mathcal{O}_2 &= \frac{g_2^2}{2\Lambda^2} H^\dagger H W^a_{\mu\nu} W^{a\mu\nu}, \\
\tilde{\mathcal{O}}_2 &= \frac{g_2^2}{2\Lambda^2} H^\dagger H W^a_{\mu\nu} \tilde{W}^{a\mu\nu}, \\
\mathcal{O}_{12} &= \frac{g_1 g_2}{2\Lambda^2} H^\dagger \tau^a H B_{\mu\nu} W^{a\mu\nu}, \\
\tilde{\mathcal{O}}_{12} &= \frac{g_1 g_2}{2\Lambda^2} H^\dagger \tau^a H B_{\mu\nu} \tilde{W}^{a\mu\nu}, \\
\mathcal{O}_3 &= \frac{g_3^2}{2\Lambda^2} H^\dagger H G^A_{\mu\nu} G^{A\mu\nu}, \\
\tilde{\mathcal{O}}_3 &= \frac{g_3^2}{2\Lambda^2} H^\dagger H G^A_{\mu\nu} \tilde{G}^{A\mu\nu},
\end{aligned} \tag{2.2}$$

where the dual field strength tensor is defined as $\tilde{F}_{\mu\nu} = \frac{1}{2}\epsilon_{\mu\nu\lambda\sigma} F^{\lambda\sigma}$ $(F = B, W, G)$ and the others are in the standard notations. Note that we have absorbed the SM gauge couplings and the cutoff Λ into the definition of the operators. The operator $\mathcal{O}_{12}$ gives the direct $SU(2)$-$U(1)_Y$ gauge mixing and modifies the oblique parameter S [34] at the tree level [33],

$$\triangle S = \frac{8\pi v^2}{\Lambda^2} c_{12}, \tag{2.3}$$

when the two Higgs fields are replaced by their vacuum expectation values (VEVs). The current S parameter bound, $S = 0.00^{+0.11}_{-0.10}$ [35], already sets a strong limit on c_{12}. Similarly, the $\tilde{\mathcal{O}}_3$ operator yields an effective QCD θ_{QCD}-term and thus $\tilde{c}_3$ is strongly constrained by the neutron EDM. Therefore, we will set $c_{12} = \tilde{c}_3 = 0$ in our global analysis, which will be discussed in the numerical section.

There are three more dim-6 gauge-Higgs operators that give rise to the tree-level modification to the coupling between Higgs and gauge fields:

$$(D_\mu H)^\dagger (D_\nu H) B^{\mu\nu},$$
$$(D^\mu H)^\dagger \sigma^a (D^\nu H) W^a_{\mu\nu}, \tag{2.4}$$
$$|H^\dagger D_\nu H|^2.$$

However, these operators are severely constrained by electroweak precision tests; for example, the SM gauge boson mass matrix will be altered by these operators at tree level. Since we are focusing on the Higgs physics at the LHC and it is safe to ignore these operators, we confine our analysis with six out of the eight gauge-Higgs operators given in Eq. (2.2).

The relevant $hV^\mu(k_1)V'^\nu(k_2)$ Feynman rules are summarized in Table I, where (k_1, k_2) are the 4-momentum carried by the gauge bosons and (μ, ν) are the corresponding Lorentz indices. The two gauge-invariant form factors are defined as

$$S^{\mu\nu}(k_1, k_2) = k_2^\mu k_1^\nu - k_1 \cdot k_2 g^{\mu\nu},$$
$$P^{\mu\nu}(k_1, k_2) = \epsilon^{\alpha\beta\mu\nu} k_{1\alpha} k_{2\beta}. \tag{2.5}$$

Also, we define

$$a_1 \equiv c_1 + c_2 - c_{12} \simeq c_1 + c_2,$$
$$\tilde{a}_1 \equiv \tilde{c}_1 + \tilde{c}_2 - \tilde{c}_{12},$$
$$a_2 \equiv s_{2W}\left(c_2 - c_1 t_W^2 - \frac{1}{2} c_{12}(1 - t_W^2)\right) \simeq s_{2W}(c_2 - c_1 t_W^2),$$
$$\tilde{a}_2 \equiv s_{2W}\left(\tilde{c}_2 - \tilde{c}_1 t_W^2 - \frac{1}{2} \tilde{c}_{12}(1 - t_W^2)\right),$$
$$a_4 \equiv c_W^2(c_2 + c_1 t_W^4 + c_{12} t_W^2) \simeq c_W^2(c_2 + c_1 t_W^4),$$
$$\tilde{a}_4 \equiv c_W^2(\tilde{c}_2 + \tilde{c}_1 t_W^4 + \tilde{c}_{12} t_W^2), \tag{2.6}$$

where $\sin\theta_W$ is denoted as s_W for notational convenience. Similarly, we adopt the following abbreviations: $\cos\theta_W \to c_W$, $\sin 2\theta_W \to s_{2W}$, $\tan\theta_W \to t_W$, etc. From Table I, one can easily obtain the corresponding $hhVV'$ Feynman rules by replacing the VEV, v, by the Higgs field. Because of the non-Abelian nature of $SU(2)_L$, the operators $\mathcal{O}_2$, $\tilde{\mathcal{O}}_{2,12}$ also give rise to the tree-level γWW coupling when both SM Higgs fields take their VEVs. The extra γWW interaction has been overlooked in the previous studies. However, it gives nonzero contributions to the fermion EDM and $(g-2)$. Explicitly, after electroweak spontaneous symmetry breaking, the relevant Lagrangian is

$$\delta\mathcal{L}_{\gamma VV} = c_2 g_2^2 \frac{v^2}{4\Lambda^2} W^a_{\mu\nu} W^{a,\mu\nu} + \tilde{c}_2 g_2^2 \frac{v^2}{4\Lambda^2} W^a_{\mu\nu} \tilde{W}^{a,\mu\nu} - \tilde{c}_{12} g_1 g_2 \frac{v^2}{4\Lambda^2} B_{\mu\nu} \tilde{W}^{3,\mu\nu}. \tag{2.7}$$

The $\tilde{c}_2$ term is equivalent to a total derivative that has no effect in the local perturbation calculation. The c_2 term modifies the canonical normalization of the kinematic term of $SU(2)$ gauge fields. Thus the c_2-corresponding γWW form factor is same as in the SM, but the coupling is now the SM one times $-c_2 g_2^2 v^2/\Lambda^2$.

For the triple $\gamma^\alpha(k_1) W^{+,\beta}(k_2) W^{-,\lambda}(k_3)$ coupling, where all three momenta are entering the vertex, the corresponding Feynman rules for $\tilde{c}_{12}$ can be spelled out:

$$\tilde{\Gamma}_6^{\alpha\beta\lambda} = i \frac{g_2^3 s_W v^2}{2\Lambda^2} \tilde{c}_{12} \epsilon^{\mu\alpha\beta\lambda} k_{1\mu}. \tag{2.8}$$

TABLE I. Feynman rules for the $hV^\mu(k_1)V'^\nu(k_2)$ vertices, where (k_1, k_2) are entering the vertices.

	$S^{\mu\nu}(k_1, k_2)$	$P^{\mu\nu}(k_1, k_2)$
$h\gamma\gamma$	$i\frac{2vg_2^2 s_W^2}{\Lambda^2} a_1$	$i\frac{2vg_2^2 s_W^2}{\Lambda^2} \tilde{a}_1$
$h\gamma Z$	$i\frac{vg_2^2}{\Lambda^2} a_2$	$i\frac{vg_2^2}{\Lambda^2} \tilde{a}_2$
hgg	$i\frac{2vg_3^2}{\Lambda^2} c_3$	$i\frac{2vg_3^2}{\Lambda^2} \tilde{c}_3 \simeq 0$
hZZ	$i\frac{2vg_2^2}{\Lambda^2} a_4$	$i\frac{2vg_2^2}{\Lambda^2} \tilde{a}_4$
hWW	$i\frac{2vg_2^2}{\Lambda^2} c_2$	$i\frac{2vg_2^2}{\Lambda^2} \tilde{c}_2$

III. HIGGS PRODUCTION AND DECAY

The SM Higgs production cross sections and their branching ratios have been calculated and maintained by the LHC Higgs Cross Section Working Group [22]. For later convenience, we collect the SM results in Tables II and III. Note that the inherent theoretical uncertainties of the SM prediction for both Higgs production and decays range from a few percents to about $\sim 20\%$.

Both CP-even and CP-odd operators affect the Higgs production and decay at tree level, and the two kinds of contributions do not mix. It is useful to define the following ratios to characterize different production and decay channels of the SM Higgs

$$\alpha_{ij} = \frac{\Gamma(h \to ij)}{\Gamma^{\rm SM}(h \to ij)}, \qquad \gamma_{XY} = \frac{\sigma(XY \to h)}{\sigma^{\rm SM}(XY \to h)}, \tag{3.1}$$

where (i, j) and (X, Y) stand for the final states and the initial particles respectively. At tree-level, the gauge-Higgs operators have no effects on the SM Yukawa couplings so that $\alpha_{ff} = 1$. Since the gluon-gluon fusion(GF) is the dominate contribution to the Higgs production at LHC, for simplicity we will ignore the change to the other production channels due to the presence of the gauge-Higgs operators. Next, we discuss how the gauge-Higgs operators modify γ_{gg} and the relevant α_{ij}.

A. Gluon fusion

The effective operators that describe short-distance features will not change the gluon parton distribution function and kinematics, so we just need to focus on the partonic cross section, which is

TABLE II. Cross sections of the SM Higgs boson at 125 GeV [22], where WH and ZH stand for the associated production with W and Z, respectively. The uncertainties are shown in percentages.

σ (pb)			
	LHC 7 TeV (%)	LHC 8 TeV (%)	LHC 14 TeV (%)
GF	$15.32^{+14.7}_{-14.9}$	$19.52^{+14.7}_{-14.7}$	$49.85^{+19.6}_{-14.6}$
VBF	$1.205^{+2.7}_{-2.4}$	$1.578^{+2.8}_{-3.0}$	$4.180^{+2.8}_{-3.0}$
WH	$0.5729^{+3.7}_{-4.3}$	$0.6966^{+3.7}_{-4.1}$	$1.504^{+4.1}_{-4.4}$
ZH	$0.3158^{+4.9}_{-5.1}$	$0.3943^{+5.1}_{-5.0}$	$0.8830^{+6.4}_{-5.5}$

TABLE III. Branching ratios of different decay channels for the SM Higgs boson at 125 GeV [22]. The uncertainties are shown in percentages.

$10^2 \times \mathcal{B}(h \to ij)$							
bb (%)	cc (%)	$\tau\tau$ (%)	$\gamma\gamma$ (%)	ZZ (%)	WW (%)	gg (%)	γZ (%)
$57.7^{+3.2}_{-3.3}$	$2.91^{+12.2}_{-12.2}$	$6.32^{+5.7}_{-5.7}$	$0.228^{+5.0}_{-4.9}$	$2.64^{+4.3}_{-4.2}$	$21.5^{+4.3}_{-4.2}$	$8.57^{+10.2}_{-10.0}$	$0.154^{+9.0}_{-8.8}$

$$\hat{\sigma}_{\rm LO}(gg \to h) = \sigma_0^h m_h^2 \delta(\hat{s} - m_h^2) = \frac{\pi^2}{8m_h}\Gamma(h \to gg)\delta(\hat{s} - m_h^2). \quad (3.2)$$

Then, the ratio of the cross section is

$$\gamma_{gg} \equiv \frac{\hat{\sigma}(gg \to h)}{\hat{\sigma}_{\rm SM}(gg \to h)} = \frac{\Gamma(h \to gg)}{\Gamma_{\rm SM}(h \to gg)}. \quad (3.3)$$

In the SM, the Higgs decays to two gluons via a heavy quark loop, and the decay width is well-known [36],

$$\Gamma(h \to gg) = \frac{G_F \alpha_s^2 m_h^3}{64\sqrt{2}\pi^3}|A_{\frac{1}{2}}(\tau_t)|^2, \quad (3.4)$$

where $\tau_t = \frac{m_h^2}{4m_t^2}$ and $A_{\frac{1}{2}}$ is given by

$$A_{\frac{1}{2}}(\tau) = 2[\tau + (\tau - 1)f(\tau)]\tau^{-2},$$
$$f(\tau) = \begin{cases} \arcsin^2\sqrt{\tau} & \tau \le 1 \\ -\frac{1}{4}\left[\ln\frac{1+\sqrt{1-\tau^{-1}}}{1-\sqrt{1-\tau^{-1}}} - i\pi\right]^2 & \tau > 1 \end{cases}. \quad (3.5)$$

Incorporating the CP-even and CP-odd effective operator contributions, the total decay width can be calculated to be

$$\Gamma(h \to gg) = \frac{G_F \alpha_s^2 m_h^3}{64\sqrt{2}\pi^3}\left(\left|A_{\frac{1}{2}}(\tau_t) + \frac{16\sqrt{2}\pi^2}{G_F\Lambda^2}c_3\right|^2 + \left|\frac{16\sqrt{2}\pi^2}{G_F\Lambda^2}\tilde{c}_3\right|^2\right), \quad (3.6)$$

which agrees with Ref. [29]. But as already stated, the $\tilde{c}_3$ is severely constrained by the neutron EDM; only the CP-even operator $\mathcal{O}_3$ is relevant to the ratio of the gluon-gluon fusion cross section,

$$\gamma_{gg} = \left|1 + \frac{16\sqrt{2}\pi^2}{G_F\Lambda^2 A_{\frac{1}{2}}(\tau_t)}c_3\right|^2. \quad (3.7)$$

B. Diphoton decay

The $h \to 2\gamma$ decay width relates to the amplitude

$$\Gamma = \frac{1}{32\pi m_h}|\mathcal{M}^{\gamma\gamma}|^2, \quad (3.8)$$

where

$$\mathcal{M}^{\gamma\gamma} = \mathcal{M}_{\rm SM}^{h\to\gamma\gamma} + \frac{2vg_2^2 s_W^2}{\Lambda^2}a_1 S^{\alpha\beta}(k_1, k_2)\epsilon_{1\alpha}^*\epsilon_{2\beta}^* + \frac{2vg_2^2 s_W^2}{\Lambda^2}\tilde{a}_1 P^{\alpha\beta}(k_1, k_2)\epsilon_{1\alpha}^*\epsilon_{2\beta}^*, \quad (3.9)$$

with the SM contribution [36,37]

$$\mathcal{M}_{\rm SM}^{h\to\gamma\gamma} = M_1 S_{\mu\nu}(k_1, k_2)\epsilon_1^{\mu*}\epsilon_2^{\nu*}, \quad M_1 = \frac{\alpha}{2\pi}(\sqrt{2}G_F)^{\frac{1}{2}}\left(A_1(\tau_W) + \frac{4}{3}A_{\frac{1}{2}}(\tau_t)\right), \quad (3.10)$$

where $A_{\frac{1}{2}}$ is from top quark loop as given in the GF section and A_1 is from the W boson loop,

$$A_1(\tau) = -[2\tau^2 + 3\tau + 3(2\tau - 1)f(\tau)]\tau^{-2}, \quad (3.11)$$

and parameter $\tau_i = \frac{m_h^2}{4m_i^2}$. It is straightforward to calculate the ratio of decay rates:

$$\alpha_{\gamma\gamma} = \frac{|\mathcal{M}(h\to\gamma\gamma)|^2}{|\mathcal{M}_{\rm SM}(h\to\gamma\gamma)|^2} = \left|1+\frac{8\sqrt{2}\pi^2 a_1}{G_F\Lambda^2[A_1(\tau_W)+\frac{4}{3}A_{\frac{1}{2}}(\tau_t)]}\right|^2 + \left|\frac{8\sqrt{2}\pi^2\tilde{a}_1}{G_F\Lambda^2[A_1(\tau_W)+\frac{4}{3}A_{\frac{1}{2}}(\tau_t)]}\right|^2. \quad (3.12)$$

C. $h\to\gamma Z$

The decay rate for $h\to\gamma Z$ in the rest frame of the Higgs boson is

$$\Gamma = \frac{1}{16\pi m_h}\left(1-\frac{m_Z^2}{m_h^2}\right)|\mathcal{M}^{\gamma Z}|^2. \quad (3.13)$$

The amplitude including high-dimensional operators' contributions is

$$\mathcal{M}^{\gamma Z} = \mathcal{M}_{\rm SM}^{(h\to\gamma Z)} + \frac{vg_2^2}{\Lambda^2}a_2 S^{\mu\nu}\epsilon^*_{1\mu}\epsilon^*_{2\nu} + \frac{vg_2^2}{\Lambda^2}\tilde{a}_2 P^{\mu\nu}\epsilon^*_{1\alpha}\epsilon^*_{2\beta}, \quad (3.14)$$

and the SM contribution [36,38,39] is given as

$$\begin{aligned}\mathcal{M}_{\rm SM}^{(h\to\gamma Z)} &= M_2 S^{\mu\nu}\epsilon^*_{1\mu}\epsilon^*_{2\nu},\\ M_2 &= \frac{\alpha}{2\pi}(\sqrt{2}G_F)^{\frac{1}{2}}(A_F+A_W),\\ A_F &= -\frac{2\hat{v}_t}{c_W s_W}A_{\frac{1}{2}}^{\gamma Z}(\tau_t,\lambda_t),\\ A_W &= -\frac{1}{s_W}A_1^{\gamma Z}(\tau_W,\lambda_W),\end{aligned} \quad (3.15)$$

where $\tau_i = \frac{m_h^2}{4m_i^2}$, $\lambda_i = \frac{m_Z^2}{4m_i^2}$ (i $= t$, W) and fermion vector coupling $\hat{v}_f = 2I_f^3 - 4Q_f s_W^2$. The relevant functions are

$$\begin{aligned}A_{\frac{1}{2}}^{\gamma Z}(\tau,\lambda) &= [I_1(\tau,\lambda)-I_2(\tau,\lambda)],\\ A_1^{\gamma Z}(\tau,\lambda) &= c_W\{4(3-t_W^2)I_2(\tau,\lambda)+[(1+2\tau)t_W^2 - (5+2\tau)]I_1(\tau,\lambda)\},\\ I_1(\tau,\lambda) &= \frac{1}{2(\lambda-\tau)}+\frac{1}{2(\lambda-\tau)^2}[f(\tau)-f(\lambda)] + \frac{\lambda}{(\lambda-\tau)^2}[g(\tau)-g(\lambda)],\\ I_2(\tau,\lambda) &= -\frac{1}{2(\lambda-\tau)}[f(\tau)-f(\lambda)],\\ g(\tau) &= \begin{cases}\sqrt{\tau^{-1}-1}\arcsin\sqrt{\tau} & \tau<1\\ \frac{\sqrt{1-\tau^{-1}}}{2}\left[\ln\frac{1+\sqrt{1-\tau^{-1}}}{1-\sqrt{1-\tau^{-1}}}-i\pi\right] & \tau\geq 1\end{cases}.\end{aligned} \quad (3.16)$$

Then, the ratio of the decay rates is

$$\alpha_{\gamma Z} = \frac{|\mathcal{M}(h\to\gamma Z)|^2}{|\mathcal{M}_{\rm SM}(h\to\gamma Z)|^2} = \left|1+\frac{8\sqrt{2}\pi^2 a_2}{G_F\Lambda^2(A_F+A_W)}\right|^2 + \left|\frac{8\sqrt{2}\pi^2\tilde{a}_2}{G_F\Lambda^2(A_F+A_W)}\right|^2. \quad (3.17)$$

D. $h\to WW^*, ZZ^*$

Unlike the cases of $h\to gg$, $\gamma\gamma$, γZ, which are 1-loop processes in the SM, the leading contributions to $h\to WW^*$, ZZ^* start at tree level in the SM. Moreover, the SM tree-level $hV^\mu V^\nu$ vertex is $\sim g^{\mu\nu}$, which mixes nontrivially with the form factor $S^{\mu\nu}$ when squaring the amplitude. So, $\alpha_{WW,ZZ}$ cannot be expressed as $|1+\epsilon c_{\rm even}|^2+|\epsilon' c_{\rm odd}|^2$, where ϵ, ϵ' are some small numbers, as in the previous cases. To obtain the $h\to VV^*(V=W,Z)$ decay, one needs to perform a straightforward tree-level calculation and take care of the phase-space integration of the 3-body final state. When the decay final states of the gauge boson V^* are massless, the expression can be largely simplified but is still not very illustrating. The details can be found in the Appendix. With the presence of the gauge-Higgs operators, the ratio of $h\to VV^*$ decay rates is

$$\begin{aligned}\alpha_{WW} &= \frac{R_1(m_W/m_h,a_W)}{R_1(m_W/m_h,0)}+\tilde{c}_2^2\frac{32m_h^2m_W^2}{\Lambda^4}\frac{R_2(m_W/m_h)}{R_1(m_W/m_h,0)},\\ \alpha_{ZZ} &= \frac{R_1(m_Z/m_h,a_Z)}{R_1(m_Z/m_h,0)}+\tilde{a}_4^2\frac{32m_h^2m_Z^2c_W^4}{\Lambda^4}\frac{R_2(m_Z/m_h)}{R_1(m_Z/m_h,0)},\end{aligned} \quad (3.18)$$

where the relevant CP-even NP is encoded by two parameters:

$$a_W = \frac{8m_W^2}{\Lambda^2}c_2, \qquad a_Z = \frac{8m_W^2}{\Lambda^2}a_4.$$

Our results for $\alpha_{gg,\gamma\gamma,\gamma Z}$ agree with Ref. [29], and the explicit expression for $\alpha_{WW,ZZ}$ is, however, new. Now, we are fully equipped for the later numerical analysis on the LHC Higgs decay data.

E. Numerical expressions for α's

Taking $\Lambda = 1$ TeV as a reference point, numerically, we have

$$\begin{aligned}
\alpha_{gg} &= \gamma_{gg} = (1 + 13.90c_3)^2, \\
\alpha_{\gamma\gamma} &= [1 - 1.48(c_1 + c_2)]^2 + 2.18(\tilde{c}_1 + \tilde{c}_2 - \tilde{c}_{12})^2, \\
\alpha_{\gamma Z} &= [1 + 0.46c_1 - 1.54c_2]^2 + 0.71[0.55\tilde{c}_1 \\
&\quad - 1.82\tilde{c}_2 + 0.64\tilde{c}_{12}]^2, \\
\alpha_{WW} &= 1 - 0.019c_2 + 1.3 \times 10^{-4}c_2^2 + 5.2 \times 10^{-5}\tilde{c}_2^2, \\
\alpha_{ZZ} &= 1 - 0.86 \times 10^{-3}c_1 - 0.0096c_2 + 2.6 \times 10^{-7}c_1^2 \\
&\quad + 5.8 \times 10^{-6}c_1c_2 + 3.0 \times 10^{-5}c_2^2 \\
&\quad + 1.3 \times 10^{-5}(\tilde{c}_2 + 0.09\tilde{c}_1 + 0.28\tilde{c}_{12})^2. \qquad (3.19)
\end{aligned}$$

By rescaling $c_i \to c_i \times (\Lambda/1\ \mathrm{TeV})^2$, one can easily obtain the numerical expression for the cutoff scale, which differs from 1 TeV. Since the $h \to \gamma\gamma$, $Z\gamma$, gg are the loop precesses in the SM, these modes are more sensitive to the NP. One can see that the prefactors associated with c's and $\tilde{c}$'s in $\alpha_{gg,\gamma\gamma,\gamma Z}$ are all around 1.0. On the other hand, the leading contributions for $h \to WW$, ZZ begin at tree level in the SM. The NP modification to these modes is relatively 2 orders weaker, by a loop factor $\sim 1/16\pi^2$, compared to $h \to gg$, $\gamma\gamma$, γZ.

IV. EDM AND $g - 2$

First, we set our convention. The EDM of a fermion, d_f, is defined by the low-energy effective Lagrangian

$$\mathcal{L}_{\mathrm{EDM}} = -\frac{1}{2} d_f \bar{u}(p_2) i\gamma_5 \sigma_{\mu\nu} u(p_1) F^{\mu\nu}, \qquad (4.1)$$

where u and $\bar{u}$ are the spinor wave function. It is well-known that the fermion EDM starts at least at the 3-loop level for quarks and the 4-loop level for leptons in the SM. However, with the CP-odd operators in the effective Lagrangian (2.1), the fermion EDM can be generated at the one-loop level, and there are three possible contributions from the CP-odd $h\gamma\gamma$, $h\gamma Z$, and γWW interactions; see Fig. 1. We note in passing that quarks can acquire a nonvanishing chromoEDM if $\tilde{c}_3 \neq 0$. A similar consideration of using the EDM to constrain the CP-odd Wilson coefficients can be found in Refs. [27,28], in which only the contributions from Fig. 1(a) have been taken into account. As discussed in the introduction, we perform the 1-loop calculation by dimensional regularization and extract the finite part by the $\overline{\mathrm{MS}}$ scheme. Our result for the complete 1-loop contributions is summarized as

$$\begin{aligned}
d_f = -e\frac{\alpha}{\pi}\frac{m_f}{v^2}\Big[& Q_f \tilde{a}_1 K_1(\Lambda, m_h) + \tilde{a}_2 \frac{\frac{1}{2}I_f - Q_f s_W^2}{s_W^2 s_{2W}} \\
& \times K_2(\Lambda, m_Z, m_h) + \frac{\tilde{c}_{12}}{4s_W^2} K_1(\Lambda, m_W)\Big], \qquad (4.2)
\end{aligned}$$

where the definition of $\tilde{a}_1$, $\tilde{a}_2$ has been given in Eq. (2.6), I_f is the fermion's isospin, and, in our convention, $e = |e|$ and $Q_e = -1$. In the bracket, the first, second, and third terms represent the contributions from Figs. 1(a)–1(c), respectively. In the limit in which $m_f \ll m_h$, the functions $K_{1,2}$ take the form

$$\begin{aligned}
K_1(\mu, x) &\equiv \frac{v^2}{\Lambda^2}\Big[\frac{3}{4} + \frac{1}{2}\ln\frac{\mu^2}{x^2}\Big], \\
K_2(\mu, x, y) &\equiv \frac{v^2}{\Lambda^2}\Big[\frac{3}{4} + \frac{1}{2}\frac{(x^2 \ln\frac{\mu^2}{x^2} - y^2 \ln\frac{\mu^2}{y^2})}{(x^2 - y^2)}\Big],
\end{aligned} \qquad (4.3)$$

where μ is the dimensional regularization scale. A similar result for the $h\gamma\gamma$ contribution can be found in Ref. [28]; our result is different from Ref. [27] up to a finite term. For the neutron EDM, we adopt the QCD sum rule estimation

$$d_n = (1 \pm 0.5)[1.1e(\tilde{d}_d + 0.5\tilde{d}_u) + 1.4(d_d - 0.25d_u)], \qquad (4.4)$$

given in Ref. [40] to relate the quark EDM and neutron EDM.[2] We take $m_u = 2.3$ MeV, $m_d = 4.8$ MeV, and $\alpha = 1/128.0$ for our numerical study. The quark chromoEDMs are ignored due to the θ_{QCD} constraint. In terms of the Wilson coefficients, we obatin

$$\begin{aligned}
d_e &= (7.00\tilde{c}_1 + 7.39\tilde{c}_2 - 16.07\tilde{c}_{12}) \times 10^{-26}\ \mathrm{e\,cm}, \\
d_n &= (1.91\tilde{c}_1 + 10.04\tilde{c}_2 - 16.25\tilde{c}_{12}) \times 10^{-25}\ \mathrm{e\,cm}.
\end{aligned} \qquad (4.5)$$

From the latest bounds, $|d_e| < 1.05 \times 10^{-27}\mathrm{e\,cm}$ (90% C.L.) [43] and $|d_n| < 2.9 \times 10^{-26}$ e cm (90% C.L.) [44], we obtain two inequalities:

$$\begin{aligned}
&|66.69\tilde{c}_1 + 70.37\tilde{c}_2 - 153.01\tilde{c}_{12}| < 1 \quad (1.6\sigma), \\
&(1 \pm 0.5) \times |6.60\tilde{c}_1 + 34.64\tilde{c}_2 - 56.02\tilde{c}_{12}| < 1 \quad (1.6\sigma).
\end{aligned} \qquad (4.6)$$

When combining the above two conditions together, the allowed region is a solid tube with a tiny parallelogram cross section passing through the origin along the $\{0.735, 1.478, 1.0\}$ direction in the $\{\tilde{c}_1, \tilde{c}_2, \tilde{c}_{12}\}$ space.

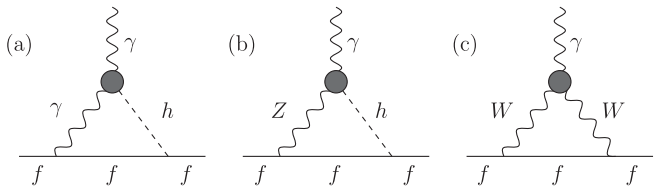

FIG. 1. The 1-loop contributions to the electron and quark EDMs and charged lepton $g - 2$. The gray bulbs represent the effective gauge-Higgs operators. Note that the mirror image diagrams are not displayed.

[2] In principle, when RG running is taken into account, one gets a better estimation of the neutron EDM. See Ref. [41] for the discussion of the RG running of dimension-5, dim-6 CP-odd operators and the bound on the left-right model scale from the neutron EDM. For a recent study on the RG running of dim-6 CP-odd operators and the neutron EDM bound, see Ref. [42].

The same 1-loop diagrams in Fig. 1 with CP-even operators give rise to a_f, the anomalous magnetic dipole moment (AMDM) of charged leptons. The AMDM can be extracted from the charged lepton's photon form factor,

$$i\mathcal{M} = ie\bar{u}(p_2)\left[\gamma^\mu F_1(q^2) + \frac{i\sigma^{\mu\nu}q_\nu}{2m}F_2(q^2)\right]u(p_1),$$
$$a_f \equiv \frac{g-2}{2} = F_2(0), \tag{4.7}$$

where the momentum transfer $q = p_2 - p_1$. Again, we perform the 1-loop calculation, in the unitary gauge, with dimensional regularization and in the $\overline{\text{MS}}$ scheme. We obtain the following result:

$$a_f = -\frac{\alpha}{\pi}\frac{m_f^2}{v^2}\left[2a_1 Q_f K_1(\Lambda, m_h) + 2a_2\frac{\frac{1}{2}I_f - Q_f s_W^2}{s_W^2 s_{2W}} \times K_2(\Lambda, m_Z, m_h) + \frac{5}{6}\frac{c_2 v^2}{s_W^2\Lambda^2}\right]. \tag{4.8}$$

The first and second term in the bracket are the finite parts of Figs. 1(a) and 1(b), respectively. The third term, which has no divergence, stems from the effective dimension-4 $(WW\gamma)$ interaction introduced by the operator $\mathcal{O}_2$. The contribution to a_f from this new $(WW\gamma)$ interaction can be obtained by multiplying the factor $-(c_2 g_2^2 v^2/\Lambda^2)$ with the well-known SM $WW\gamma$ contribution [45]. Numerically, we obtain $\Delta a_\mu = 1.61(c_1 + 0.41c_2)\times 10^{-10}$ for $\Lambda = 1$ TeV.

For the charged lepton anomalous magnetic diploe moment, the deviation of the experimental measurement from the SM prediction [35,46,47] is

$$\Delta a_\mu = a_\mu^{\text{exp}} - a_\mu^{\text{SM}} = (2.39 \pm 0.79)\times 10^{-9}(1\sigma),$$
$$\Delta a_e = a_e^{\text{exp}} - a_e^{\text{SM}} = -10.6(8.1)\times 10^{-13}(1\sigma). \tag{4.9}$$

Since the gauge-Higgs operators are flavor blind, the resulting Δa_f scales as m_f^2 so $\Delta a_e = (m_e/m_\mu)^2\Delta a_\mu$. Assuming that $\Delta a_{e,\mu}$ are solely attributed to the gauge-Higgs operators and using the latest data, Eq. (4.9), we obtain a best fit at $\Delta a_\mu = 2.37\times 10^{-9}$ from the least-square fit, and

$$c_1 + 0.41c_2 = 15.25 \pm 5.09. \tag{4.10}$$

The allowed region is basically a wide infinite strip away from the origin on the c_1-c_2 plane.

V. NUMERICAL ANALYSIS

To quantify how each Higgs decay channel differs from its SM prediction at the LHC, we follow Ref. [48] and use the signal strength parameter $\hat{\mu}$, which is defined as

$$\hat{\mu}_{ij} = \frac{\sigma(X\to h)\mathcal{B}(h\to ij)}{\sigma(X\to h)_{\text{SM}}\mathcal{B}(h\to ij)_{\text{SM}}}, \tag{5.1}$$

where X stands for the initial partons in the proton and i, j represent the decay products. The branching fractions are given by $\mathcal{B}_{ij} \equiv \mathcal{B}(h\to ij) = \Gamma_{ij}/\Gamma_{\text{tot}}$, and Γ_{tot} is the actual total Higgs decay width. The Γ_{tot} is related to the SM prediction by $\Gamma_{\text{tot}} = C_{\text{tot}}\Gamma_{\text{tot}}^{\text{SM}}$. Then, in terms of α's and $\mathcal{B}$'s, C_{tot} can be expressed as the sum of all contributions from the major decay channels,

$$\begin{aligned} C_{\text{tot}} &\sim \mathcal{B}_{bb}^{\text{SM}} + \mathcal{B}_{\tau\tau}^{\text{SM}} + \mathcal{B}_{cc}^{\text{SM}} + \alpha_{\gamma\gamma}\mathcal{B}_{\gamma\gamma}^{\text{SM}} + \alpha_{gg}\mathcal{B}_{gg}^{\text{SM}} \\ &\quad + \alpha_{WW}\mathcal{B}_{WW}^{\text{SM}} + \alpha_{ZZ}\mathcal{B}_{ZZ}^{\text{SM}} + \alpha_{Z\gamma}\mathcal{B}_{Z\gamma}^{\text{SM}} \\ &\sim 0.67 + 0.0023\alpha_{\gamma\gamma} + 0.086\gamma_{gg} + 0.026\alpha_{ZZ} \\ &\quad + 0.215\alpha_{WW} + 0.0015\alpha_{Z\gamma}, \end{aligned} \tag{5.2}$$

where the SM branching ratios for a 125 GeV Higgs are adopted from Ref. [22] and we note that $\alpha_{ff} = 1$ at tree level since the gauge-Higgs operators do not modify the Yukawa interactions. Because of the parton distribution function, the loop-induced gluon fusion is the dominant production mechanism ($\sim$ 87–88%) at the LHC for a Higgs with mass around 125 GeV. And among all production channels, it is the most sensitive to new physics. Therefore, it is a fairly good approximation to take $\sigma(gg\to h)/\sigma(gg\to h)_{\text{SM}} \sim \gamma_{gg}$. Therefore, we have

$$\hat{\mu}_{ij} \sim \frac{\gamma_{gg}\alpha_{ij}}{C_{\text{tot}}}. \tag{5.3}$$

As the common practice, a function χ^2 is defined for multiparameters fitting

$$\chi^2 = \sum_i \frac{(\hat{\mu}_i - \bar{\mu}_i)^2}{\delta_i^2}, \tag{5.4}$$

where $\bar{\mu}_i$ is the mean experimental value, δ_i is the combined uncertainty from both the experimental and theoretical sides, and $\hat{\mu}_i$ is the theoretic prediction either from a specific model or determined by the effective gauge-Higgs operators. We use the most updated Higgs data collected and analyzed by the ATLAS and CMS groups, see Table IV. Since we explicitly take $\sigma(gg\to h)/\sigma(gg\to h)_{\text{SM}} \sim \gamma_{gg} = \alpha_{gg}$, in the CMS $h\to ZZ^*$ channels, we only use the gluon-gluon fusion data. We drop $\bar{\mu}_{bb}$ from the global fitting for both groups have large uncertainties and both are via the VH production.

A. Pseudoglobal fit of ATLAS and CMS results

To proceed, we first treat the five α's in Eq. (5.2) as mutually independent free parameters and conduct a pseudoglobal fit by using the current LHC data listed in Table IV. The best fit is located at

$$\gamma_{gg}^{\text{LHC}} = 0.99, \quad \alpha_{\gamma\gamma}^{\text{LHC}} = 1.26, \quad \alpha_{WW}^{\text{LHC}} = 0.84, \quad \alpha_{ZZ}^{\text{LHC}} = 1.30, \quad \alpha_{Z\gamma}^{\text{LHC}} = 1.00, \tag{5.5}$$

with minimum $\chi_0^2 = 4.94$, and the 1σ boundary corresponds to the contour of $\chi_{1\sigma}^2 = \chi_0^2 + 5.89$ for a five-parameters fit. And the 1σ model-independent correlations

TABLE IV. The signal strength $\bar{\mu}$ from Moriond 2013.

$\bar{\mu}_{ij}$	CMS	ATLAS
ZZ^*	$0.91^{+0.30}_{-0.24}$ (inclusive) $1.0^{+2.4}_{-2.3}$ (qqH, VH) $0.9^{+0.5}_{-0.4}$ (GF) [13,17]	$1.7^{+0.5}_{-0.4}$ (inclusive) [3,9]
WW^*	$0.76^{+0.21}_{-0.21}$ (inclusive) [13,18]	1.01 ± 0.31 (inclusive) [4,10]
$\gamma\gamma$	$0.78^{+0.28}_{-0.26}$ (MVA) $1.11^{+0.32}_{-0.30}$ (cut based) [14,16]	$1.65^{+0.34}_{-0.30}$ (inclusive) [3,8]
γZ	<9 [20]	<18.2 [3,7]
bb	HCP12: $1.3^{+0.7}_{-0.6}$ (VH) [6]	$1.09 \pm 0.20 \pm 0.22$ (VH) [5,12]
$\tau\tau$	$1.1^{+0.4}_{-0.4}$ (inclusive) [15,19]	0.7 ± 0.7 (inclusive) [6,11]

between α_{ij} and γ_{gg} are displayed in Fig. 2. Basically, the message from doing this trivial exercise is clear and simple: (1) The current LHC data more or less agree with the SM, and (2) the larger the Higgs gluon-gluon fusion production, the smaller the Higgs decay widths and vice versa. We see that the global fit prefers a SM-like Higgs gluon fusion production. However, this still introduces a degenerate solution to c_3, $(1 + 13.92c_3) = \pm\sqrt{1.0 \pm 0.7}$. And the two corresponding 1σ allowed regions for c_3 are $\in [-0.167, -0.114]$ and $\in [-0.029, 0.023]$. This degeneracy for c_3 also inevitably exists in the later global fitting. We will discuss how to lift this degeneracy phenomenologically in Sec. VI.

B. Limits on the gauge-Higgs Wilson coefficient by using the Higgs data alone

Next, we do the global fit by using the current LHC data in terms of $c_{1,2,3}$ and $\tilde{c}_{1,2,12}$. For a 6-dimensional parameter fitting, the 95% C.L. (68% C.L.) contour corresponds to $\chi^2_{95(68)} = \chi^2_{\rm min} + 12.59(7.01)$. To have an idea how the Wilson coefficients will be constrained when the experimental sensitivity is improved and eventually compatible with the SM theoretical uncertainties, we also consider a "fake" data set that all signal strengths equal one, $\bar{\mu} = 1.0$. And we take the combined SM theoretical uncertainties, $\sigma_{\rm SM} = \sqrt{\sigma^2_{\rm BR} + \sigma^2_{\rm GF}}$, from Tables II and III, as the "experimental" errors. The 95% C.L. results are shown in Fig. 3. Some features of our results are as follows:

(1) The CP-even Wilson coefficients are well-constrained by the current LHC data. The LHC limits on c_1, c_2, and c_3 are basically compatible, around two times bigger, with the benchmark experimental sensitivity by using the SM theoretical predictions and uncertainties as input.

(2) On the other hand, the constraints on the CP-odd Wilson coefficients $\tilde{c}_{1,2,12}$ are poor by using the Higgs decays data alone. However, they seem to fall on a long line segment in the parameter space. This linear relation can be easily understood as roughly the solution to make the CP-odd contributions vanish simultaneously in $\alpha_{\gamma\gamma}$ and $\alpha_{\gamma Z}$, Eq. (3.19), since the two are most sensitive to the presence of CP-odd contributions.

The most important message from this drill is that there still is the allowance for NP with $c_{1,2} \sim$ a few and $\tilde{c}$'s $\sim \mathcal{O}(100)$ for $\Lambda = 1$ TeV hiding in the SM theoretical uncertainties.

Interestingly, from our numerical study, we find a linear correlation among α_{WW} vs α_{ZZ} and the signal strength μ_{WW} vs μ_{ZZ}; see Fig. 4. Our results show that at 95% C.L., $\alpha_{ZZ} \sim 1.5\alpha_{WW}$ and $1.0 \lesssim \alpha_{ZZ} \lesssim 1.6$. However, when converted to signal strength, it becomes $\mu_{ZZ} \sim \mu_{WW}$ and $0.6 \lesssim \mu_{ZZ,WW} \lesssim 1.4$. The best-fit values for both cases are SM-like.

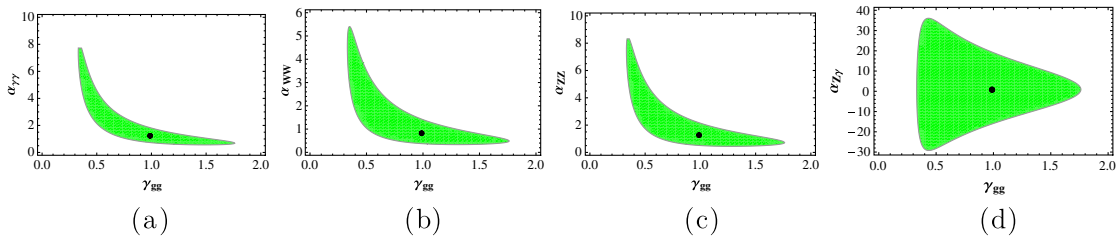

FIG. 2 (color online). The 1σ correlations between: (a) $\alpha_{\gamma\gamma}$ and γ_{gg}, (b) α_{WW} and γ_{gg}, (c) α_{ZZ} and γ_{gg}, and (d) $\alpha_{\gamma Z}$ and γ_{gg}. The best-fit locations are marked by dots.

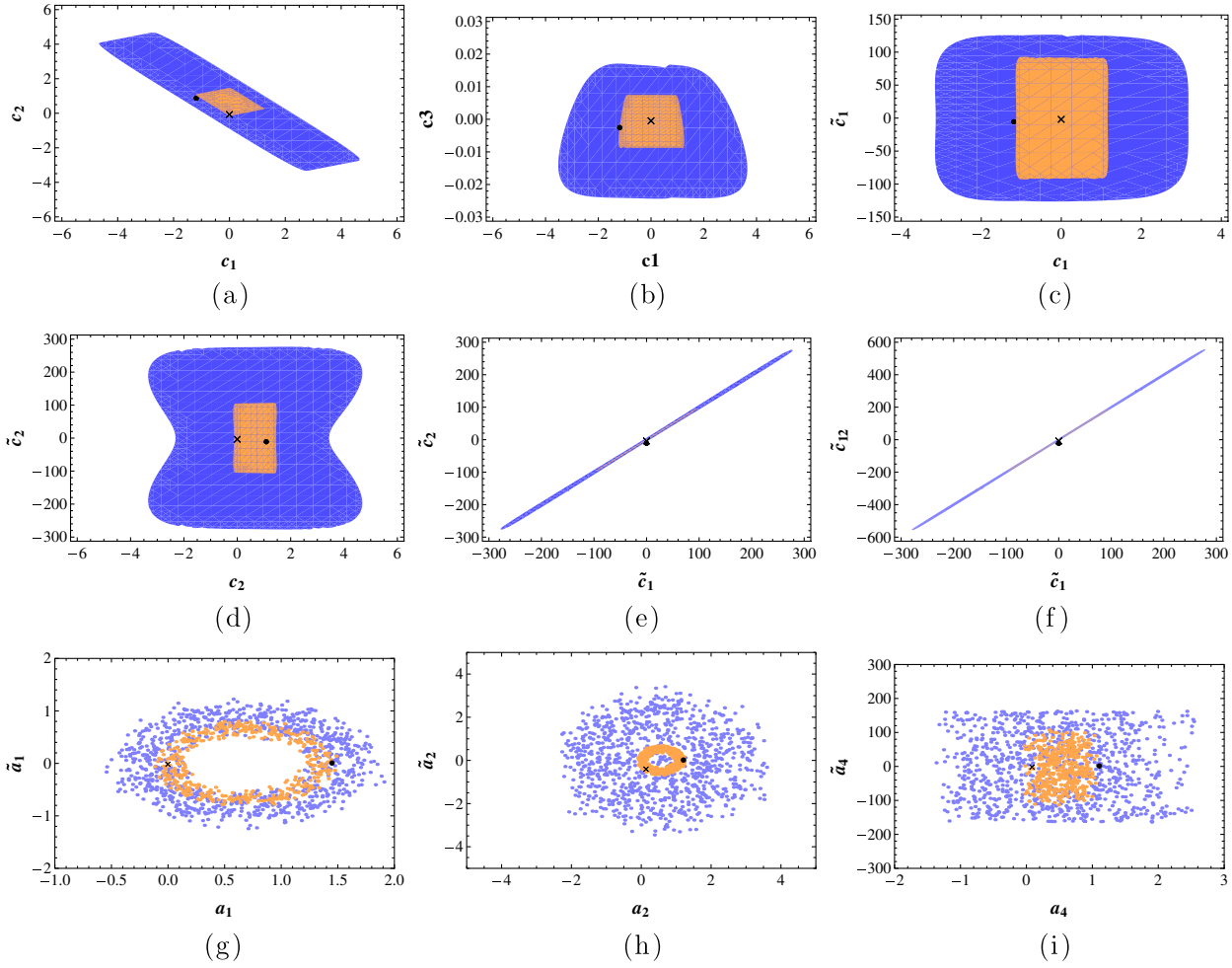

FIG. 3 (color online). The 95% C.L. allowed region in (a–f) the Wilson coefficient space, and (g–i) the hVV couplings, by using the LHC data (blue/darker) and the SM predictions(light brown/lighter). The best fit location is shown at the dot(cross) for LHC data (SM). The minimum $\chi^2 = 6.413(0.0)$ for LHC data(SM). In subdiagram(b), we only display the SM like allowed region for c_3.

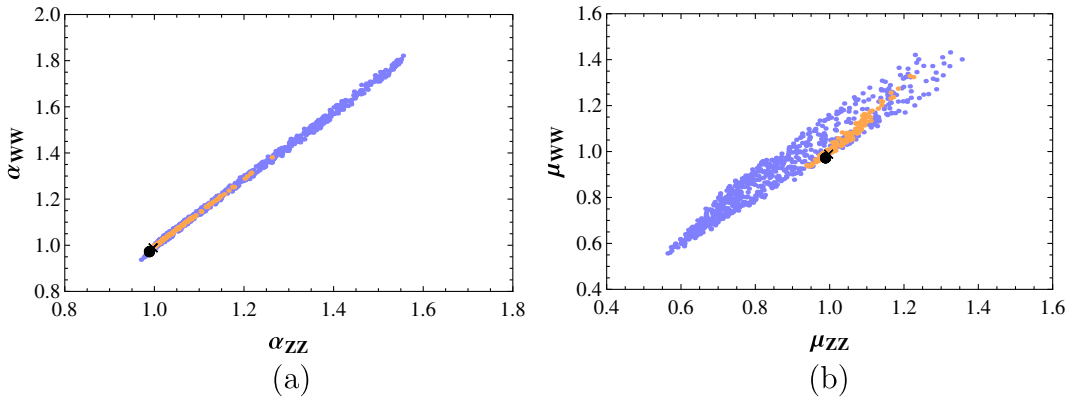

FIG. 4 (color online). The 95% C.L. correlations between the $h \to WW^*$ and $h \to ZZ^*$ decay rate ratios, subdiagram (a), and signal strength, subdiagram (b). The best-fit point is marked by the dot/cross, and the blue (darker)/ brown (lighter) region is used for the LHC/SM data.

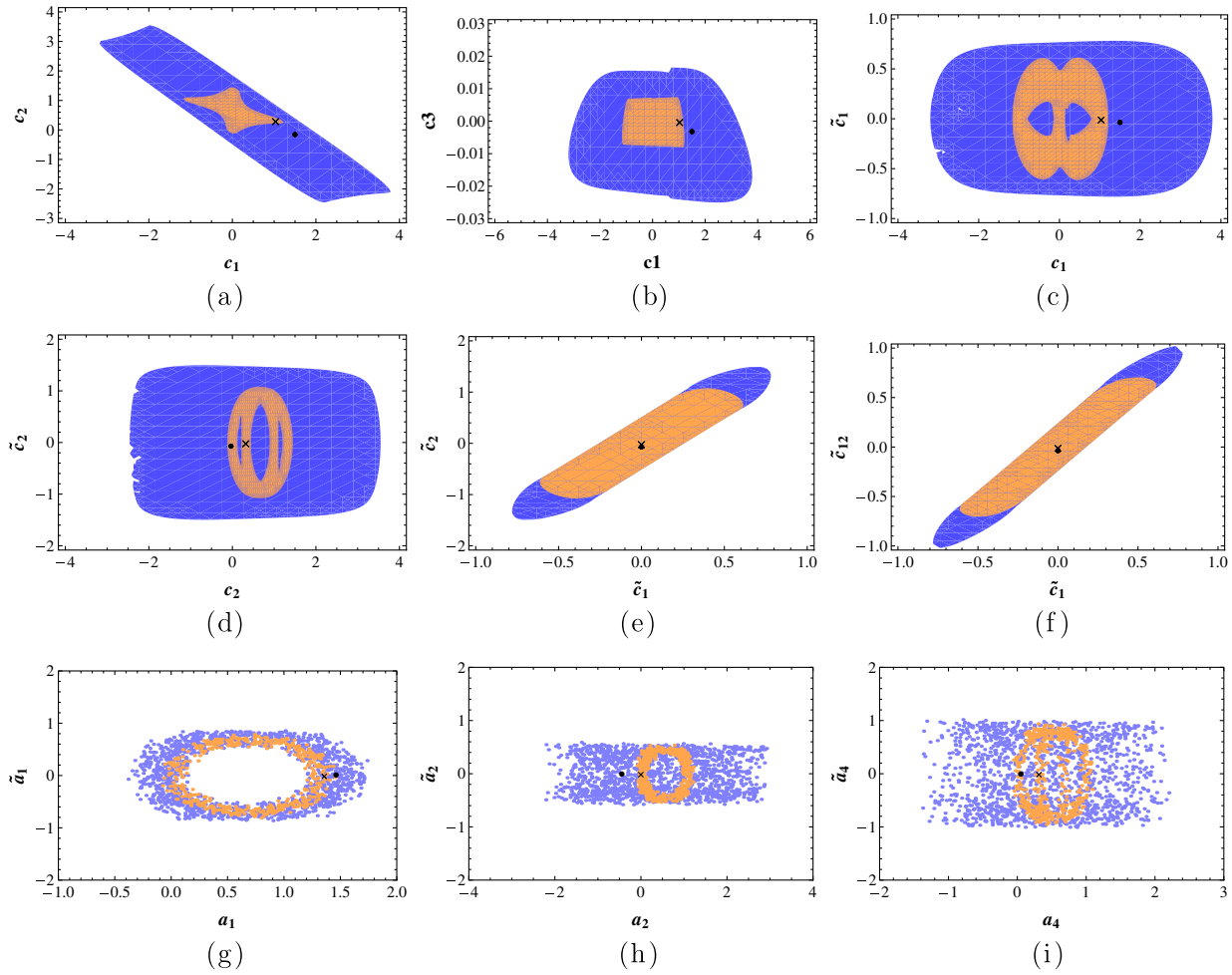

FIG. 5 (color online). The 95% C.L. allowed region in (a–f) the Wilson coefficient space and (g–i) in the Higgs-gauge couplings space by using Higgs data, the EDM, and the AMDM. The blue (darker) and light brown (lighter) regions are for using the LHC data and SM predictions, respectively. The best-fit location is shown at the dot (cross) for LHC data (SM). The corresponding minimum $\chi^2 = 15.89(9.63)$ for LHC data (SM). In subdiagram (b), only the SM-like c_3 region is shown.

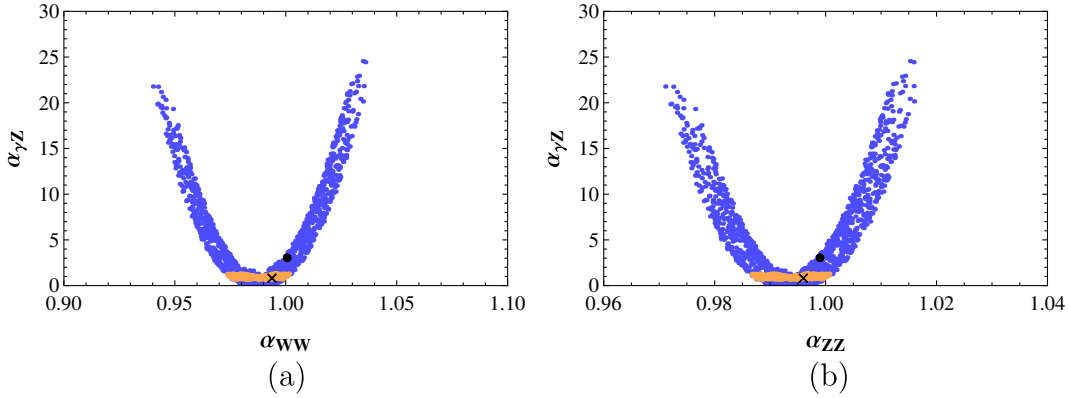

FIG. 6 (color online). The 95% C.L. decay rate ratios correlation between (a) $h \to WW$ and $h \to \gamma Z$ and (b) $h \to ZZ$ and $h \to \gamma Z$. The best-fit point is marked by the dot/cross, and the blue (darker)/brown (lighter) region is for using the LHC/SM data.

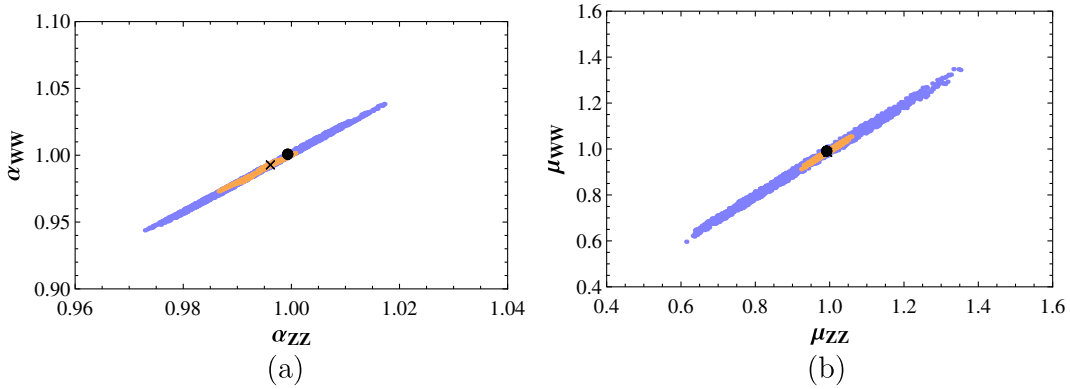

FIG. 7 (color online). This plot is similar to Fig. 4 but with additional constraints from EDMs and AMDMs.

C. Constraints on the gauge-Higgs Wilson coefficient by using the Higgs data plus EMDs and AMDMs

Finally, we include four more data points, d_e, d_n, $\triangle a_e$, and $\triangle a_\mu$, into the global fitting. And the 95% C.L. results are shown in Fig. 5. One can clearly see that, when the electron and neutron EDM are included in the global fitting, the limits on the CP-odd Wilson coefficients are dramatically improved. Even giving extra, say $\sim\mathcal{O}(10)$, uncertainties to the 1-loop EDM estimations by using the effective operators, the inclusion of EDMs into the analysis still plays an important role to limit the CP properties of the 125 GeV boson. More implications of including the EDM constraints will be discussed in Sec. VI C.

Some interesting correlations emerge among $\alpha_{\gamma Z,ZZ,WW}$; see Figs. 6 and 7(a). Roughly, we observe that

$$\begin{aligned}(\alpha_{WW}-1) &\sim 2(\alpha_{ZZ}-1),\\ (\alpha_{\gamma Z}-1) &\sim 6.5\times 10^3(\alpha_{WW}-1)^2\\ &\sim 2.57\times 10^4(\alpha_{ZZ}-1)^2.\end{aligned} \tag{5.6}$$

These relations can be easily understood. Since the EDMs strongly constrain the CP-odd Wilson coefficients, the α's will be dominated by the CP-even Wilson coefficients c_1 and c_2. From Eq. (3.19), we see that $\alpha_{\gamma Z,WW,ZZ}$ are more sensitive to c_2 than c_1; thus, the approximate relations follow. However, when translated into the signal strength, only the relation between μ_{ZZ} and μ_{WW} holds; see Fig. 7(b). Therefore, we find that $\mu_{ZZ}\sim\mu_{WW}$ and $0.6\lesssim\mu_{ZZ,WW}\lesssim 1.4$ are quite robust with or without taking EDM constraints into account. Better than $\lesssim 1\%$ accuracy of determination the individual absolute Higgs decay width is required to test the relations given in Eq. (5.6). This will be very challenging at the LHC but could be done at the precision Higgs machines in the future.

VI. DISCUSSION AND CONCLUSION

A. Discriminate the degenerate solutions

From the global fit of the latest LHC Higgs data, in the presence of effective gauge-Higgs operators, we obtain $\gamma_{gg}\simeq 1.0\pm 0.4$. This introduces a degenerate solution to c_3, $1+13.92c_3=\pm\sqrt{1.0\pm 0.4}$. One solution is SM-like with c_3 centers around zero. Another possible solution, $c_3\sim -0.14$, corresponds to the fact that the NP gluon-gluon fusion amplitude equals minus two times the SM amplitude. We would like to point out that this degeneracy can be easily lifted once the LHC has enough Higgs pair production data in the high-luminosity phase. The Higgs pair production by gluon-gluon fusion in the SM, $G^\mu(p_a)G^\nu(p_b)\to h(p_c)h(p_d)$, has been analyzed in Ref. [49] and summarized in the review paper [36]. In the SM, the two gluons must carry the same color, and this process receives contributions from the triangle diagram and box diagram. Both diagrams yield the spin-0 form factor while the box diagram contributes an additional spin-2 form factor. The SM amplitude is

$$\begin{aligned}\mathcal{M}(G^aG^b\to H^cH^d)=\frac{G_F\alpha_s s}{2\sqrt{2}\pi}\Big[&\frac{3m_h^2}{s-m_h^2}F_T A_{0\mu\nu}\\ &+(F_B A_{0\mu\nu}+G_B A_{2\mu\nu})\Big]\epsilon_a^\mu\epsilon_b^\nu,\end{aligned} \tag{6.1}$$

where $s=(p_a+p_b)^2$ and the spin-0/2 form factors $A_0^{\mu\nu}(\propto S^{\mu\nu})/A_2^{\mu\nu}$ are given by

$$\begin{aligned}A_0^{\mu\nu}&=g^{\mu\nu}-\frac{p_a^\nu p_a^\mu}{p_a\cdot p_b},\\ A_2^{\mu\nu}&=g^{\mu\nu}+\frac{p_c^2 p_a^\nu p_b^\mu}{p_T^2(p_a\cdot p_b)}-\frac{2(p_b\cdot p_c)p_a^\nu p_c^\mu}{p_T^2(p_a\cdot p_b)}\\ &\quad-\frac{2(p_a\cdot p_c)p_b^\mu p_c^\nu}{p_T^2(p_a\cdot p_b)}+\frac{2p_c^\mu p_c^\nu}{p_T^2}.\end{aligned} \tag{6.2}$$

For more details, see Ref. [49]. The operator $\mathcal{O}_3$ provides an additional contribution to the spin-0 amplitude, and the amplitude square becomes

$$|\mathcal{M}|^2 = \frac{G_F^2 \alpha_s^2 s^2}{8\pi^2}\left(\left| \frac{3m_h^2}{s-m_h^2} F_T + F_B - \frac{8\sqrt{2}\pi^2}{G_F \Lambda^2} c_3 \right|^2 + |G_B|^2 \right). \tag{6.3}$$

If taking $\Lambda = 1$ TeV, the exotic solution, $c3 \sim -0.14$, gives $\frac{-8\sqrt{2}\pi^2}{G_F\Lambda^2} c_3 \sim +1.34$ inside the spin-0 amplitude square. Because of the cancelation between the contributions from F_T and F_B,[3] this exotic solution generates a sizable deviation from the SM prediction. Therefore, this two-fold degeneracy could be resolved by the future Higgs pair production data.

B. UV complete models

Here, we discuss and make comparisons of the validity of our effective operator analysis of two UV complete toy models. Let us first examine the model that contains an additional color octet scalar S for which the SM quantum number is (8, 2, 1/2) [33] on top of the SM. The most general scalar potential is

$$\begin{aligned} V = {} & \frac{\lambda}{4}(H^{\dagger i}H_i)^2 + 2m_S^2 \,\mathrm{Tr} S^{\dagger i} S_i + \lambda_1 H^{\dagger i} H_i \,\mathrm{Tr} S^{\dagger j} S_j + \lambda_2 H^{\dagger i} H_j \,\mathrm{Tr} S^{\dagger j} S_i \\ & + (\lambda_3 H^{\dagger i} H^{\dagger j} \,\mathrm{Tr} S_i S_j + \lambda_4 H^{\dagger i} \,\mathrm{Tr} S^{\dagger j} S_j S_i + \lambda_5 H^{\dagger i} \,\mathrm{Tr} S^{\dagger j} S_i S_j + \mathrm{H.c.}) \\ & + \lambda_6 \,\mathrm{Tr} S^{\dagger i} S_i S^{\dagger j} S_j + \lambda_7 \,\mathrm{Tr} S^{\dagger i} S_j S^{\dagger j} S_i + \lambda_8 \,\mathrm{Tr} S^{\dagger i} S_i \,\mathrm{Tr} S^{\dagger j} S_j + \lambda_9 \,\mathrm{Tr} S^{\dagger i} S_j \,\mathrm{Tr} S^{\dagger j} S_i \\ & + \lambda_{10} \,\mathrm{Tr} S_i S_j \,\mathrm{Tr} S^{\dagger i} S^{\dagger j} + \lambda_{11} \,\mathrm{Tr} S_i S_j S^{\dagger j} S^{\dagger i}, \end{aligned} \tag{6.4}$$

where i, j are the $SU(2)$ indices and m_S is the mass of the color octet scalar. The custodial symmetry requires the following relations to hold: $2\lambda_3 = \lambda_2$, $2\lambda_6 = 2\lambda_7 = \lambda_{11}$, $\lambda_9 = \lambda_{10}$ for the real couplings [33] and $\lambda_4 = \lambda_5^*$ for the complex ones [50]. And the SM quarks can now couple to both H and S by

$$\begin{aligned} -\mathcal{L}_Y = {} & y_{ij}^U \bar{Q}_{Li} \tilde{H} u_{Rj} + y_{ij}^D \bar{Q}_{Li} H d_{Rj} + Y_{ij}^U \bar{Q}_{Li} \tilde{S}^A T^A u_{Rj} \\ & + Y_{ij}^D \bar{Q}_{Li} S^A T^A d_{Rj} + \mathrm{H.c.}, \end{aligned} \tag{6.5}$$

where T^A is the $SU(3)$ generator and A is the color index. The Yukawa couplings y and Y are, in general, complex. In Fig. 8 we show how we can generate these effective gauge-Higgs operators. One typical diagram to produce CP-even operator is Fig. 8(a), which is at one-loop level. Based on a naive dimensional analysis, the Wilson coefficients are given [33]:

$$\frac{c_3}{\Lambda^2} = \frac{3}{2}\frac{c_2}{\Lambda^2} = \frac{3}{2}\frac{c_1}{\Lambda^2} = \frac{2\lambda_1 + \lambda_2}{64\pi^2 m_S^2}, \qquad \frac{c_{12}}{\Lambda^2} = \frac{\lambda_2}{48\pi^2 m_S^2}. \tag{6.6}$$

And the CP-violating operators are generated at the two-loop level; see Fig. 8(b). A ballpark estimation gives

$$\frac{\tilde{c}_{1,2,12,3}}{\Lambda^2} \sim \sum_{i,j} \frac{\mathrm{Im}[u_{ij}^* v_{ij}]}{(16\pi^2)^2} \frac{m_{q_i} m_{q_j}}{m_S^2 \max\{m_{q_{i,j}}^2, m_H^2\}}, \tag{6.7}$$

where $q_{i,j}$ are in the mass basis and the octet Yukawas are parameterized as $\bar{q}_i T^A (u_{ij} + v_{ij}\gamma^5) q_j S^A$. Even though the CP-violating phase is of order 1, the strength of the $\tilde{c}$'s are roughly 2 orders smaller than the CP-even Wilson coefficients in this model.

Since this model is UV complete, we are able to discuss the fermion EDM and AMDM at above the electroweak scale without encountering any divergence. The charged lepton $(g-2)$ starts at the two-loop level; see Figs. 9(a) and 9(b).[4] Both Figs. 9(a) and 9(b) can be related to the diagram shown in Fig. 8(a) by substituting VEV(s) for either one or two of the external H legs. And this is exactly what we have performed in the gauge-Higgs operator analysis for $\triangle a_e$ and $\triangle a_\mu$.

For the most general Yukawa coupling, Eq. (6.5), SM quarks receive a nonzero EDM at the 2-loop level; see Figs. 9(c) and 9(d).[5] Both Figs. 9(c) and 9(d) are independent of Fig. 8(b), and our gauge-Higgs operator estimations for quark EDMs are subleading. On the other hand, there are two kinds of contributions to the SM lepton EDM: (1) 3-loop diagrams, by connecting Fig. 8(b) to the lepton line by either the SM Higgs or gauge bosons. These leading contributions have been taken care of by our gauge-Higgs operator analysis. (2) 4-loop diagrams, first by joining the two external quark lines to form a loop in Figs. 9(c) or 9(d), and then connecting the resulting bulb to the lepton lines via either SM Higgs or gauge bosons. These are 4-loop diagrams. So our gauge-Higgs operator estimation for lepton EDMs are indeed the leading contribution. Nevertheless, in the case that Yukawa couplings are most general, one needs to incorporate the Fermion EDM/AMDM effective operators in the analysis; see Ref. [53] for an earlier study on the interplay of the four-fermion operators and the electric and magnetic diploe operators.

To avoid the flavor-changing neutral current and other phenomenological problems, it is a common practice to

[3] In the large quark mass limit, $F_T = \frac{2}{3} + \mathcal{O}(s/m_Q^2)$, $F_B = -\frac{2}{3} + \mathcal{O}(s/m_Q^2)$, and $G_B = \mathcal{O}(s/m_Q^2)$ [49].

[4] The resulting 2-loop $(g-2)$ can be read and translated from Ref. [51], in which the similar diagrams due to exotic scalars have been considered.

[5] The formulas in Ref. [52], in which EDMs are generated via the similar diagrams in supersymmetry models, can be easily translated for use in this octet model.

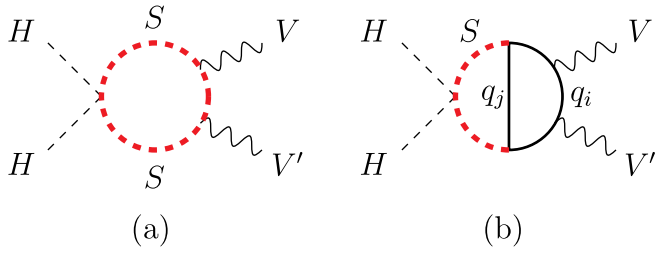

FIG. 8 (color online). Some typical loop diagrams that generate the effective gauge-Higgs operators in the color octet scalar model. Where S's, the red (thick) dashed lines, are the color octet scalars, q's are the SM quarks, H is the SM Higgs doublet, and V and V' are the SM vector bosons. Note there are many other ways to attach the V and V' if gauge symmetry allowed. Diagram (a) is the leading contribution to the CP-even gauge-Higgs operators. The CP-odd gauge-Higgs operators begin at the two-loop level, diagram (b).

assume that $Y_{ij}^{U/D} = \beta^{U/D} y_{ij}^{U/D}$, where $\beta^{U/D}$ are real. In that case, both Yukawas are real in the fermion mass basis, and the contributions from Figs. 9(c) and 9(d) vanish. However, the CP-violating gauge-Higgs operators, Fig. 8(b), vanish as well, and we do not have any say about the CP-violation constraint. Assuming that $\Lambda = m_S = 1$ TeV, our numerical study gives $-3 \lesssim c_1 \lesssim 4$, $-2.5 \lesssim c_2 \lesssim 3$, $-0.25 \lesssim c_{12} \lesssim 0.25$ (from the S parameter) and $-0.02 \lesssim c_3 \lesssim 0.015$; if we take the SM-like solution, then

$$-118 \lesssim \lambda_2 \lesssim 118, \qquad -12.6 \lesssim 2\lambda_1 + \lambda_2 \lesssim 9.5. \quad (6.8)$$

In addition to the positivity conditions for the scalar potential, Eq. (6.4), the above limits provide further nontrivial constrains on the parameter space of this model.

Based on the above discussion, one can tailor a modified UV-complete model in which our gauge-Higgs operator analysis is applicable. In one of the modified versions, the octet scalar is replaced by a real $SU(2)$ triplet, S_t, which carries the SM quantum number (8, 3, 0). Because of the $SU(2)$ representation, it has no Yukawa couplings to all SM fermions, and thus there is neither flavor-changing neutral current problems nor the EDM contributions from Figs. 9(c) and 9(d). The most general renormalizable potential of the octet-triplet scalar is

$$\begin{aligned} V(S_t) = {} & \frac{\lambda}{4}(H^\dagger H)^2 + m_{S_t}^2 \,\mathrm{Tr}(S_t^i S_t^i) + i\mu_t \epsilon^{ijk} \,\mathrm{Tr}(S_t^i S_t^j S_t^k) \\ & + \lambda_{t1} H^\dagger H \,\mathrm{Tr}(S_t^i S_t^i) + \lambda_{t2} \,\mathrm{Tr}(S_t^i S_t^i S_t^j S_t^j) \\ & + \lambda_{t3} \,\mathrm{Tr}(S_t^i S_t^j S_t^i S_t^j) + \lambda_{t4} \,\mathrm{Tr}(S_t^i S_t^i) \,\mathrm{Tr}(S_t^j S_t^j) \\ & + \lambda_{t5} \,\mathrm{Tr}(S_t^i S_t^j) \,\mathrm{Tr}(S_t^i S_t^j), \end{aligned} \quad (6.9)$$

where $i, j, k = 1, 2, 3$ are the $SU(2)$ indices for adjoint representation. Moreover, we introduce a pair of exotic vector fermions, $\psi_{L,R}$, for which the SM quantum numbers are $(6, 2, 1/2)$. The vector fermions admit a Dirac mass and a Yukawa coupling to S_t,

$$\mathcal{L} \supset m_\psi \bar{\psi}_L \psi_R + \eta_t \bar{\psi}_L S_t \psi_R + \mathrm{H.c.} \quad (6.10)$$

The Dirac mass m_ψ is taken to be real without losing any generality and assumed to be much larger than v so that the exotic fermions decouple as S_t does when energy is below the electroweak scale. The Yukawa η_t is complex, in general. The CP-violating gauge-Higgs operators can be generated at two-loop levels, by replacing $(S, q) \to (S_t, \psi)$ in Fig. 8(b), and a rough estimation for the Wilson coefficients are

$$\frac{\tilde{c}_{1,2,12,3}}{\Lambda^2} \sim \frac{1}{(16\pi^2)^2} \frac{\mathrm{Re}\,\eta_t \,\mathrm{Im}\,\eta_t}{\max\{m_{S_t}^2, m_\psi^2\}}. \quad (6.11)$$

For $m_{S_t} \sim m_\psi \sim 1$ TeV, the θ_{QCD} gives the strongest constraint that $|\eta_t|^2 |\sin 2\theta_t| < 1.01 \times 10^{-6}$. The CP-even Wilson coefficients are generated at the 1-loop level [by replacing S by S_t in Fig. 8(a)],

$$\frac{4}{3}\frac{c_3}{\Lambda^2} = \frac{3}{4}\frac{c_2}{\Lambda^2} = \frac{\lambda_{t1}}{16\pi^2 m_{S_t}^2}, \quad (6.12)$$

but nonzero c_1 and c_{12} need to be generated at the higher-loop level since S_t carries no hypercharge. And our global fit yields that $-4.2 \le \lambda_{t1} \le 3.2$.

C. Predictions for the CP-odd decays

The spin and parity of the 125 GeV boson have been largely determined to be $J^P = 0^+$ from the analysis of the polar angular distribution in the $h \to 2\gamma$ mode [8,16] (for spin) and the polarization correlation in the $h \to ZZ \to 4l$

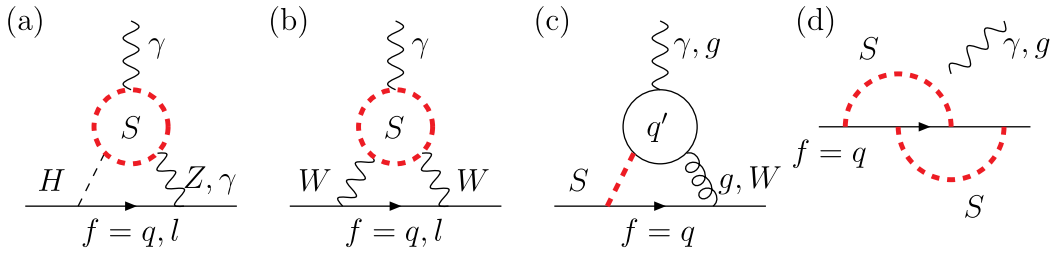

FIG. 9 (color online). Some typical leading loop diagrams that generate quark or lepton AMDMs, (a) and (b), and quark EDMs and chromoEDM, (c) and (d), in the color octet scalar model. S's, the red (thick) dashed lines, are the color octet scalars, and f is the SM fermion, either lepton or quark. Note there are many other ways to attach the external photon if gauge symmetry allowed.

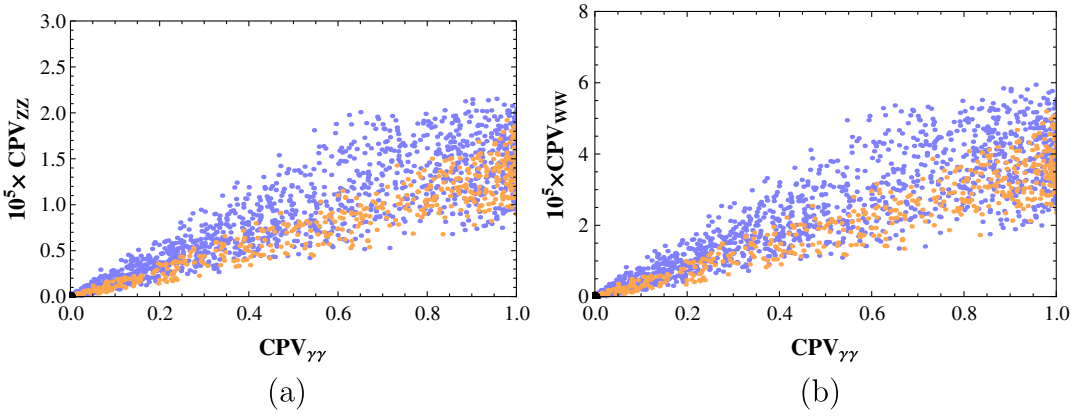

FIG. 10 (color online). The 95% C.L. *CP*-violation fraction correlations between (a) $h \to ZZ$ and $h \to \gamma\gamma$ and (b) $h \to WW$ and $h \to \gamma\gamma$. The constraints are from EDMs, AMDMs, and the LHC data (blue, darker) or SM predictions (brown, lighter).

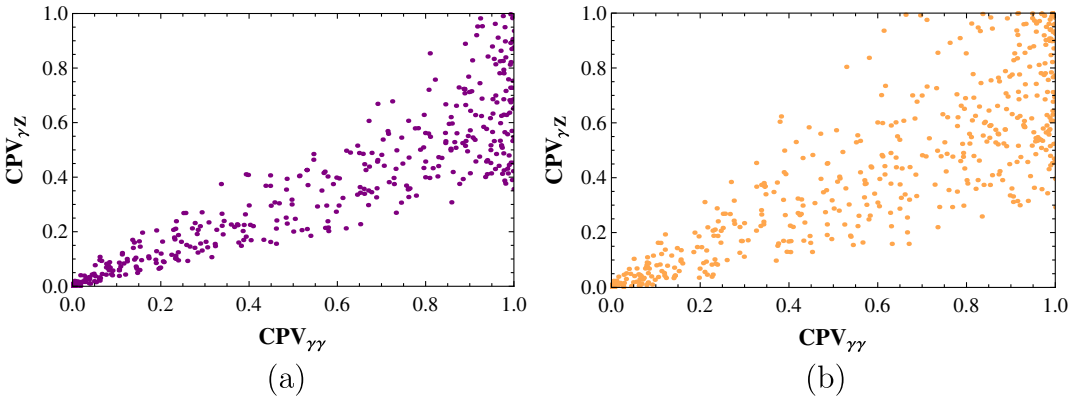

FIG. 11 (color online). (a) The 68% C.L. and (b) the 95% C.L. *CP*-violation fraction correlations between $h \to \gamma\gamma$ and $h \to \gamma Z$. The constraints are from EDMs, AMDMs, and the SM predictions.

decay [9,17] (for parity). However, the current spin-parity analyses are all based on a limited number of events and simple working assumptions; namely, the boson is assumed to be either purely scalar, pseudoscalar, a spin-2 object, etc. But we have to keep in mind that even though the 125 GeV boson is an elementary scalar, the *CP*-violation decays can still be generated by quantum corrections. For a given model, whether we have the required experimental sensitivity to detect the *CP*-odd composition is the question.

If at low energy the new physics can be indeed described by the gauge-Higgs operators alone, our numerical study predicts interesting model-independent relations among the Higgs *CP*-odd decay modes. As was discussed in Sec. IV, also in Figs. 5(e) and 5(f), the three *CP*-odd Wilson coefficients follow a linear relation on a line segment with end points at $\tilde{c}_{12}^2 \sim 0.56/1.0$ for using the SM predictions/ LHC data as input. For $\Lambda = 1$ TeV, we have [c.f. Eq. (3.19)]

$$\alpha_{\gamma\gamma}^{CP} \sim 3.21\tilde{c}_{12}^2, \quad \alpha_{\gamma Z}^{CP} \sim 1.92\tilde{c}_{12}^2, \quad \alpha_{ZZ}^{CP} \sim 4.3\times 10^{-5}\tilde{c}_{12}^2, \quad \alpha_{WW}^{CP} \sim 1.13\times 10^{-4}\tilde{c}_{12}^2. \tag{6.13}$$

Note that both $h \to WW$ and $h \to ZZ$ channels are not sensitive to the presence of the *CP*-odd gauge-Higgs operators.

We are interested in the *CP*-violation fraction, $\mathrm{CPV}_{ij} = \Gamma_{C/P}^{ij}/\Gamma^{ij}$, which is more relevant for the parity determination. In Fig. 10, we show the 95% C.L. *CP*-violation fraction correlations between (a) $h \to ZZ$ and $h \to \gamma\gamma$ and (b) $h \to WW$ and $h \to \gamma\gamma$. Note the possible large CP-violating fractions due to the gauge-Higgs effective operators in the $h \to \gamma\gamma$ and $h \to \gamma Z$ modes, which are not constrained at all by the global fit.

Apparently, it is not likely to probe the *CP*-violation fractions, at the level of $\lesssim$ (a few) $\times 10^{-5}$, in the $h \to WW$, ZZ channels at the LHC.[6] This agrees with the current parity determination results [9,17]. And, hypothetically, any future observation of the approximately few percent level *CP*-violation fraction in the $h \to ZZ$ mode will definitely indicate the existence of new physics

[6]See Ref. [54] for other proposals of measuring the *CP* nature of the Higgs at the LHC.

beyond the gauge-Higgs sector, and additional effective operators must be included.

For making use of $h \to 2\gamma$, γZ channels to probe the CP-odd components of the 125 GeV boson, we need to study the vector boson spin correlation. This could be neatly done in the future e^+e^-, $e\gamma$, or $\gamma\gamma$ colliders; see, for example, Ref. [55]. For that we have a model-independent prediction: $\alpha_{CP}^{\gamma\gamma}:\alpha_{CP}^{\gamma Z} \sim 1.67{:}1$. However, as shown in Fig. 11, when the above relation is converted into the CP-violating fraction, the relation is smeared but more or less follows a linear relation. From the plot, the CP-violating fraction correlation between these two modes is roughly

$$\mathrm{CPV}_{\gamma z} \sim (0.65 \pm 0.35)\mathrm{CPV}_{\gamma\gamma} \qquad (68\%\ \mathrm{C.L.}). \tag{6.14}$$

However, the slope becomes (0.92 ± 0.7) for the 95% C.L. fit. Although not very predictive, this prediction can be checked once the experimental sensitivities meet the SM theoretical uncertainties and the CP-violating fractions in $\gamma\gamma$ and γZ modes are measured in the future.

Nevertheless, from our numerical study, we found potentially large CP-violating compositions in the $h \to \gamma\gamma$, γZ decays.

D. Summary

We have studied the new physics associated with the 125 GeV boson for which the NP is assumed to be characterized by the effective gauge-Higgs operators. By global fitting, we studied the correlations among various Higgs to diboson decay modes. In addition to the updated Higgs measurements accumulated at the LHC, we also considered the case in which the experimental sensitivities are compatible with the SM theoretical uncertainties. We found that there is plenty of room for new physics to hide in the shadow of the inherent SM theoretical uncertainties. From the global fit, we found a robust prediction that $\mu_{ZZ} \simeq \mu_{WW}$ and $0.6 \lesssim \mu_{ZZ,WW} \lesssim 1.4$ at 95% C.L.; see Figs. 4 and 7. This can be tested at the LHC with more data in the near future.

Moreover, we take into account the constraints of EDMs and AMDMs under the assumption that the gauge-Higgs operators give the dominate contributions to them. We found very strong constraints on the CP-odd Wilson coefficients, and our numerical study indicated that the CP-violating hVV interactions in the $h \to WW$ and $h \to ZZ$ modes are too small, $\sim\mathcal{O}(10^{-5})$ at most, to be detected at the LHC; see Fig. 10. However, the CP-odd fraction in the $h\gamma\gamma$ and $h\gamma Z$ channels could be as large as $\mathcal{O}(1)$.

Two more intriguing relations are predicted if the EDM constraints are included: (1) $(\alpha_{WW} - 1) \sim 2(\alpha_{ZZ} - 1)$ and (2) $(\alpha_{\gamma Z} - 1) \sim 6500(\alpha_{WW} - 1)^2$. These predictions could be tested at the future precision Higgs machines.

The caveats are that we should keep in mind that our results are valid only for the class of NP which manifests itself in the form of the gauge-Higgs operators discussed in this work. So, our results are not applicable if (1) the existence of any light exotic degree of freedom below the electroweak scale that interacts with the Higgs boson or (2) the NP is beyond the realm that can be largely charted by the gauge-Higgs operators. On the other hand, any violation of our above predictions will indicate that the new physics must go beyond the gauge-Higgs sector.

ACKNOWLEDGMENTS

This work was supported by the Taiwan NSC, Grant No. 99-2112-M-007-006-MY3. F. X. is also supported by the Taiwan NSC, Grant No. 101-2811-M-007-051.

APPENDIX: DECAY WIDTH OF $h \to WW^*, ZZ^*$

Details of calculating the width of $h \to VV^*$ $(V = W, Z)$ are collected in this section. We consider the case that the virtute gauge boson V^* subsequently decays into two fermions f and f' with their momentums labeled as $h(P) \to V(p_1) + f(p_2) + f'(p_3)$. In the center-of-mass frame of f and f', the three-body decay width is given by the following phase integral:

$$\Gamma = \frac{1}{256\pi^3 m_h^3}\int_{(m_2+m_3)^2}^{(M-m_1)^2} ds_1 \int_{s_{2-}}^{s_{2+}} ds_2(|\mathcal{M}_1|^2 + |\mathcal{M}_2|^2), \tag{A1}$$

$$\begin{aligned} s_{2\pm} &= m_1^2 + m_3^2 + \frac{1}{2s_1}[(s - s_1 - m_1^2)(s_1 + m_3^2 - m_2^2) \\ &\quad \pm \lambda^{\frac{1}{2}}(s_1, m_3^2, m_2^2)\lambda^{\frac{1}{2}}(s_1, M^2, m_1^2)], \\ \lambda(a,b,c) &\equiv a^2 + b^2 + c^2 - 2ab - 2ac - 2bc, \end{aligned} \tag{A2}$$

where the kinematical variables are defined as $s = P^2$, $p_4 \equiv (p_2 + p_3)$, $s_1 = p_4^2$, $s_2 = (p_1 + p_3)^2$, and $s_3 = (p_1 + p_2)^2$ and $\mathcal{M}_1$ and $\mathcal{M}_2$ are the CP-even and CP-odd amplitudes, respectively. The phase space integral is largely simplified when the final-state fermions are massless, which is a good approximation in our case.

Besides the SM contribution, the CP-even amplitude also receives contributions from $\mathcal{O}_1$ and $\mathcal{O}_2$ and

$$\begin{aligned} |\mathcal{M}_1|^2 = \frac{4N_c^f(g_V^2 + g_A^2)}{(s_1 - m_V^2)^2} &\times [(m_V^2 4\sqrt{2}G_F - a_V'^2 s_1) \\ &\times (2p_1\cdot p_2 p_1\cdot p_3 - p_1^2 p_2\cdot p_3) + (m_V^2 2(\sqrt{2}G_F)^{\frac{1}{2}} \\ &- a_V' p_1\cdot p_4)^2 2p_2\cdot p_3], \end{aligned} \tag{A3}$$

where $a_W' = 2c_2 v g_2^2/\Lambda^2$, $a_Z' = 2a_4 v g_2^2/\Lambda^2$, N_c^f is the color factor of the final state fermions and $(g_V, g_A) = (g_2/2c_W)(I_3 - 2Q_f s_W^2, -I_3)$ for Z^0 and

$g_V = -g_A = g_2/2\sqrt{2}$ for $W^\pm$. And $\mathcal{M}_2$ is completely beyond the SM,

$$|\mathcal{M}_2|^2 = 8(g_V^2 + g_A^2)\left(\frac{\tilde{a}'_V}{s_1 - m_V^2}\right)^2 \times [(p_1 \cdot p_4)(p_3 \cdot p_4 p_1 \cdot p_2 + p_2 \cdot p_4 p_1 \cdot p_3) - p_4^2 p_1 \cdot p_2 p_1 \cdot p_3 - p_1^2 p_2 \cdot p_4 p_3 \cdot p_4], \quad \text{(A4)}$$

where $\tilde{a}'_W = 2\tilde{c}_2 v g_2^2/\Lambda^2$ and $\tilde{a}'_Z = 2\tilde{a}_4 v g_2^2/\Lambda^2$. Summing up all massless final states, the corresponding CP-even decay widths are

$$\Gamma_1^W = \frac{9G_F^2 m_W^4 m_h}{8\pi^3} R_1(m_W/m_h, a'_W) \quad \text{(for } W\text{)}, \qquad \Gamma_1^Z = \frac{3G_F^2 m_Z^4 m_h}{32\pi^3} \delta_Z R_1(m_Z/m_h, a'_Z) \quad \text{(for } Z\text{)}, \quad \text{(A5)}$$

with $\delta_Z = (7 - \frac{40}{3}s_W^2 + \frac{160}{9}s_W^4)$; the phase space factor R_1 will be given in below. The δ_Z factor is different from Ref. [36] and differs by a factor of 3 for the W case, but our results are consistent with Ref. [47].

For the CP-odd part, the decay widths for W and Z bosons are

$$\Gamma_2^W = \tilde{c}_2^2 \frac{9m_h^3 g_2^6 v^2}{32\pi^3\Lambda^4} R_2(\epsilon) = \tilde{c}_2^2 \frac{9G_F^2 m_W^4 m_h}{8\pi^3} \cdot \frac{32m_h^2 m_W^2}{\Lambda^4} R_2(\epsilon),$$
$$\Gamma_2^Z = \tilde{a}_4^2 \delta_Z \frac{3G_F^2 m_Z^4 m_h}{32\pi^3} \cdot \frac{32m_h^2 m_Z^2 c_W^4}{\Lambda^4} R_2(\epsilon). \quad \text{(A6)}$$

The two functions R_1, R_2 can be expressed in the form of integrals,

$$R_1(\epsilon, a'_V) \equiv \epsilon^2 \int_0^{(1-\epsilon)^2} d\tilde{s}_1 \int_{\tilde{s}_{2-}}^{\tilde{s}_{2+}} d\tilde{s}_2 \frac{1}{(\tilde{s}_1 - \epsilon^2)^2} \left\{\left(1 - \frac{a'^2_V \tilde{s}_1}{4\sqrt{2}G_F\epsilon^2}\right)\left((1 - \tilde{s}_1 - \tilde{s}_2)(\tilde{s}_2 - \epsilon^2)\frac{1}{\epsilon^2} - \tilde{s}_1\right) + 2\tilde{s}_1\left(1 - a'_V \frac{1 - \epsilon^2 - \tilde{s}_1}{4(\sqrt{2}G_F)^{\frac{1}{2}}\epsilon^2}\right)^2\right\},$$
$$R_2(\epsilon) \equiv \int_0^{(1-\epsilon)^2} d\tilde{s}_1 \int_{\tilde{s}_{2-}}^{\tilde{s}_{2+}} d\tilde{s}_2 \frac{\tilde{s}_1}{(\tilde{s}_1 - \epsilon^2)^2}\left[\frac{1}{4}(1 - \epsilon^2 - \tilde{s}_1)^2 - \frac{1}{2}\epsilon^2\tilde{s}_1 - \frac{1}{2}(\tilde{s}_2 - \epsilon^2)(1 - \tilde{s}_1 - \tilde{s}_2)\right],$$

with the relevant parameters introduced as $\epsilon = \frac{m_V}{m_h}$, $\tilde{s}_1 = \frac{s_1}{m_h^2}$, $\tilde{s}_2 = \frac{s_2}{m_h^2}$ and $\tilde{s}_{2\pm} = \frac{1}{2}(1 + \epsilon^2 - \tilde{s}_1) \pm \frac{1}{2} \times \sqrt{[(1+\epsilon)^2 - \tilde{s}_1][(1-\epsilon)^2 - \tilde{s}_1]}$. The analytical form for $R_{1,2}$ can be obtained:

$$R_1(\epsilon, a) = -\frac{1}{72\epsilon^2}\left[A + B\arctan\frac{(1-\epsilon^2)\sqrt{4\epsilon^2 - 1}}{1 - 3\epsilon^2} + C\ln\epsilon\right], \quad \text{(A7)}$$

$$A = (1-\epsilon^2)[36a\epsilon^2(-5 + 9\epsilon^2) + 6(2 - 13\epsilon^2 + 47\epsilon^4) + a^2(17 - 82\epsilon^2 + 89\epsilon^4)],$$
$$B = \frac{6}{\sqrt{4\epsilon^2 - 1}}[6(\epsilon^2 - 8\epsilon^4 + 20\epsilon^6) + 12a(\epsilon^2 - 8\epsilon^4 + 14\epsilon^6) + a^2(-1 + 11\epsilon^2 - 40\epsilon^4 + 54\epsilon^6)], \quad \text{(A8)}$$
$$C = 6[6(\epsilon^2 - 6\epsilon^4 + 4\epsilon^6) + 12a(\epsilon^2 - 6\epsilon^4 + 2\epsilon^6) + a^2(-1 + 9\epsilon^2 - 30\epsilon^4 + 6\epsilon^6)],$$
$$R_2(\epsilon) = \frac{(1-\epsilon^2)}{36}(-17 + 64\epsilon^2 + \epsilon^4) + \frac{\ln\epsilon}{6}(1 + 6\epsilon^4 - 9\epsilon^2) + \frac{(7\epsilon^2 - 1)}{6}\sqrt{4\epsilon^2 - 1}\arctan\frac{(\epsilon^2 - 1)\sqrt{4\epsilon^2 - 1}}{3\epsilon^2 - 1},$$

where

$$a \equiv \begin{cases} \frac{8m_W^2}{\Lambda^2}c_2, & \text{for } W \\ \frac{8m_W^2}{\Lambda^2}a_4, & \text{for } Z \end{cases}. \quad \text{(A9)}$$

One can check that, when $a'_V = 0$, the SM result is recovered, and $6R_1 = F(\epsilon)$ as defined in Ref. [56].

[1] ATLAS Collaboration, Phys. Lett. B **716**, 1 (2012).
[2] CMS Collaboration, Phys. Lett. B **716**, 30 (2012).
[3] F. Hubaut, in *Latest ATLAS Studies on Higgs to Diboson States, Moriond-2013, EW*, https://indico.in2p3.fr/getFile.py/access?contribId=45&sessionId=6&resId=0&materialId=slides&confId=7411.
[4] E. Mountricha, in *Study of Higgs Production in Bosonic Decay Channels at ATLAS, Moriond-2013, QCD*, http://moriond.in2p3.fr/QCD/2013/ThursdayMorning/Mountricha2.pdf.
[5] V. Martin, in *Searches for the BEH Boson into Fermions at ATLAS, Moriond-2013, EW*, https://indico.in2p3.fr/getFile.py/access?contribId=59&sessionId=6&resId=1&materialId=slides&confId=7411.
[6] D. Puigh, in *Searches for Standard Model Scalar Boson Decaying to Fermions at the LHC, Moriond-2013, QCD*, http://moriond.in2p3.fr/QCD/2013/ThursdayMorning/Puigh.pdf.
[7] ATLAS Collaboration, Report No. ATLAS-CONF-2013-009.
[8] ATLAS Collaboration, Report No. ATLAS-CONF-2013-012.
[9] ATLAS Collaboration, Report No. ATLAS-CONF-2013-013.
[10] ATLAS Collaboration, Report No. ATLAS-CONF-2013-030.
[11] ATLAS Collaboration, Report No. ATLAS-CONF-2012-160.
[12] ATLAS Collaboration, Report No. ATLAS-CONF-2012-161.
[13] G. Gómez-Ceballos, in *Study of Standard Model Scalar Production in Bosonic Decay Channels, Moriond-2013, EW*, https://indico.in2p3.fr/getFile.py/access?contribId=16&sessionId=6&resId=0&materialId=slides&confId=7411.
[14] C. Ochando, in *Study of Higgs production in Bosonic Decays Channels in CMS, Moriond-2013, QCD*, http://moriond.in2p3.fr/QCD/2013/ThursdayMorning/Ochando.pdf.
[15] V. Dutta, in *Search for the Standard Model Scalar Boson Decaying to Fermions at CMS, Moriond-2013, EW*, https://indico.in2p3.fr/getFile.py/access?contribId=57&sessionId=6&resId=0&materialId=slides&confId=7411.
[16] CMS Collaboration, Report No. CMS PAS HIG-13-001.
[17] CMS Collaboration, Report No. CMS PAS HIG-13-002.
[18] CMS Collaboration, Report No. CMS PAS HIG-13-003.
[19] CMS Collaboration, Report No. CMS PAS HIG-13-004.
[20] CMS Collaboration, Report No. CMS PAS HIG-13-006.
[21] J. Cao, Z. Heng, T. Liu, and J. M. Yang, Phys. Lett. B **703**, 462 (2011); C. Englert, T. Plehn, D. Zerwas, and P. M. Zerwas, Phys. Lett. B **703**, 298 (2011); Y. Bai, J. Fan, and J. L. Hewett, J. High Energy Phys. 08 (2012) 014; M. Carena, S. Gori, N. R. Shah, and C. E. M. Wagner, J. High Energy Phys. 03 (2012) 014; U. Ellwanger, J. High Energy Phys. 03 (2012) 044; A. Arvanitaki and G. Villadoro, J. High Energy Phys. 02 (2012) 144; B. Batell, S. Gori, and L.-T. Wang, J. High Energy Phys. 06 (2012) 172; A. Arhrib, R. Benbrik, M. Chabab, G. Moultaka, and L. Rahili, J. High Energy Phys. 04 (2012) 136; A. Arhrib, R. Benbrik, and N. Gaur, Phys. Rev. D **85**, 095021 (2012); S. Kanemura and K. Yagyu, Phys. Rev. D 85, 115009 (2012); D. Carmi, A. Falkowski, E. Kuflik, and T. Volansky, J. High Energy Phys. 07 (2012) 136; A. Azatov, R. Contino, and J. Galloway, J. High Energy Phys. 04 (2012) 127; J. R. Espinosa, C. Grojean, M. Muhlleitner, and M. Trott, J. High Energy Phys. 05 (2012) 097; P. Draper and D. McKeen, Phys. Rev. D **85**, 115023 (2012); S. Dawson and E. Furlan, Phys. Rev. D **86**, 015021 (2012); M. Carena, S. Gori, N. Shah, C. Wagner, and L.-T. Wang, J. High Energy Phys. 07 (2012) 175; A. G. Akeroyd and S. Moretti, Phys. Rev. D **86**, 035015 (2012); M. Carena, I. Low, and C. Wagner, J. High Energy Phys. 08 (2012) 060; J. A. Azatov, R. Contino, D. Del Re, J. Galloway, M. Grassi, and S. Rahatlou, J. High Energy Phys. 06 (2012) 134; M. Klute, R. Lafaye, T. Plehn, M. Rauch, and D. Zerwas, Phys. Rev. Lett. **109**, 101801 (2012); K. Kumar, R. Vega-Morales, and F. Yu, Phys. Rev. D **86**, 113002 (2012); L. Wang and X.-F. Han, Phys. Rev. D **86**, 095007 (2012); N. Bonne and G. Moreau, Phys. Lett. B **717**, 409 (2012); J. Cao, Z. Heng, J. M. Yang, and J. Zhu, J. High Energy Phys. 10 (2012) 079; W.-F. Chang, J. N. Ng, and J. M. S. Wu, Phys. Rev. D **86**, 033003 (2012); T. Corbett, O. J. P. Eboli, J. Gonzalez-Fraile, and M. C. Gonzalez-Garcia, Phys. Rev. D **86**, 075013 (2012); J. Baglio, A. Djouadi, and R. M. Godbole, Phys. Lett. B **716**, 203 (2012); M. Montull and F. Riva, J. High Energy Phys. 11 (2012) 018; J. R. Espinosa, C. Grojean, M. Muhlleitner, and M. Trott, J. High Energy Phys. 12 (2012) 045; S. Banerjee, S. Mukhopadhyay, and B. Mukhopadhyaya, J. High Energy Phys. 10 (2012) 062; A. Joglekar, P. Schwaller, and C. E. M. Wagner, J. High Energy Phys. 12 (2012) 064; F. Bonnet, T. Ota, M. Rauch, and W. Winter, Phys. Rev. D **86**, 093014 (2012); J. R. Espinosa, C. Grojean, V. Sanz, and M. Trott, J. High Energy Phys. 12 (2012) 077; B. Bellazzini, C. Petersson, and R. Torre, Phys. Rev. D **86**, 033016 (2012); J. Ke, M.-X. Luo, L.-Y. Shan, K. Wang, and L. Wang, Phys. Lett. B **718**, 1334 (2013); I. Low, J. Lykken, and G. Shaughnessy, Phys. Rev. D **86**, 093012 (2012); P. Giardino, K. Kannike, M. Raidal, and A. Strumia, Phys. Lett. B **718**, 469 (2012); M. Buckley and D. Hooper, Phys. Rev. D **86**, 075008 (2012); D. Carmi, A. Falkowski, E. Kuflik, T. Volansky, and J. Zupan, J. High Energy Phys. 10 (2012) 196; H. An, T. Liu, and L.-T. Wang, Phys. Rev. D **86**, 075030 (2012); T. Abe, N. Chen, and H.-J. He, J. High Energy Phys. 01 (2013) 082; D. Bertolini and M. McCullough, J. High Energy Phys. 12 (2012) 118; A. Joglekar, P. Schwaller, and C. Wagner, J. High Energy Phys. 12 (2012) 064; N. Arkani-Hamed, K. Blum, R. T. D'Agnolo, and J. Fan, J. High Energy Phys. 01 (2013) 149; N. Haba, K. Kaneta, Y. Mimura, and R. Takahashi, Phys. Lett. B **718**, 1441 (2013); L. G. Almeida, E. Bertuzzo, P. A. N. Machado, and R. Zukanovich Funchal, J. High Energy Phys. 11 (2012) 085; D. S. M. Alves, P. J. Fox, and N. J. Weiner, arXiv:1207.5499; B. Batell, D. McKeen, and M. Pospelov, J. High Energy Phys. 10 (2012) 104; G. Giudice, P. Paradisi, and A. Strumia, J. High Energy Phys. 10 (2012) 186; A. Delgado, G. Nardini, and M. Quiros, Phys. Rev. D **86**, 115010 (2012); J. Kearney, A. Pierce, and N. Weiner, Phys. Rev. D **86**, 113005 (2012);

M. Hashimoto and V. A. Miransky, Phys. Rev. D **86**, 095018 (2012); K. Schmidt-Hoberg and F. Staub, J. High Energy Phys. 10 (2012) 195; M. Reece, New J. Phys. **15**, 043003 (2013); H. Davoudiasl, H.-S. Lee, and W. Marciano, Phys. Rev. D **86**, 095009 (2012); Y. Cai, W. Chao, and S. Yang, J. High Energy Phys. 12 (2012) 043; K. Bae, T. Jung, and H. Kim, Phys. Rev. D **87**, 015014 (2013); M. B. Voloshin, Phys. Rev. D **86**, 093016 (2012); T. Kitahara, J. High Energy Phys. 11 (2012) 021; E. J. Chun, H. M. Lee, and P. Sharma, J. High Energy Phys. 11 (2012) 106; H. M. Lee, M. Park, and W. Park, J. High Energy Phys. 12 (2012) 037; E. Bertuzzo, P. A. N. Machado, and R. Zukanovich Funchal, J. High Energy Phys. 02 (2013) 086; B. Batell, S. Gori, and L.-T. Wang, J. High Energy Phys. 01 (2013) 139; W. Huang, J. Shu, and Y. Zhang, J. High Energy Phys. 03 (2013) 164; W. Altmannshofer, S. Gori, and G. Kribs, Phys. Rev. D **86**, 115009 (2012); G. Moreau, Phys. Rev. D **87**, 015027 (2013); C.-Q. Geng, D. Huang, Y. Tang, and Y.-L. Wu, Phys. Lett. B **719**, 164 (2013); M. Chala, J. High Energy Phys. 01 (2013) 122; I. Picek and B. Radovcic, Phys. Lett. B **719**, 404 (2013); K. Choi, S. H. Im, K. S. Jeong, and M. Yamaguchi, J. High Energy Phys. 02 (2013) 090; B. Batell, S. Jung, and H. M. Lee, J. High Energy Phys. 01 (2013) 135; K. Schmidt-Hoberg, F. Staub, and M. Winkler, J. High Energy Phys. 01 (2013) 124; H. Davoudiasl, I. Lewis, and E. Ponton, Phys. Rev. D **88**, 025017 (2013); T. Corbett, O. J. P. Eboli, J. Gonzalez-Fraile, and M. C. Gonzalez-Garcia, Phys. Rev. D **87**, 015022 (2013); M. Carena, S. Gori, I. Low, N. R. Shah, and C. E. M. Wagner, J. High Energy Phys. 02 (2013) 114; F. Arbabifar, S. Bahrami, and M. Frank, Phys. Rev. D **87**, 015020 (2013); M. Berg, I. Buchberger, D. M. Ghilencea, and C. Petersson, Phys. Rev. D **88**, 025017 (2013); G.-n. Li, G. Guo, B. Ren, Y.-J. Zheng, and X.-G. He, arXiv:1212.5528; C. Han, N. Liu, L. Wu, J. M. Yang, and Y. Zhang, arXiv:1212.6728; W. Chao, J.-H. Zhang, and Y. Zhang, J. High Energy Phys. 06 (2013) 039; S. Funatsu, H. Hatanaka, Y. Hosotani, Y. Orikasa, and T. Shimotani, Phys. Lett. B **722**, 94 (2013); J. Fan and M. Reece, J. High Energy Phys. 06 (2013) 004; P. S. Bhupal Dev, D. K. Ghosh, N. Okada, and I. Saha, arXiv:1301.3453; Phys. Rev. D **87**, 015022 (2013); J. Cao, L. Wu, P. Wu, and J. M. Yang, arXiv:1301.4641; C.-S. Chen, C.-Q. Geng, D. Huang, and L.-H. Tsai, Phys. Rev. D **87**, 075019 (2013); C. Cheung, S. D. McDermott, and K. M. Zurek, J. High Energy Phys. 04 (2013) 074; W.-Z. Feng and P. Nath, Phys. Rev. D **87**, 075018 (2013); A. Falkowski, F. Riva, and A. Urbano, arXiv:1303.1812.

[22] https://twiki.cern.ch/twiki/bin/view/LHCPhysics/CrossSections.

[23] https://twiki.cern.ch/twiki/bin/view/AtlasPublic/ExoticsPublicResults.

[24] https://twiki.cern.ch/twiki/bin/view/CMSPublic/PhysicsResultsEXO.

[25] W. Buchmüller and D. Wyler, Nucl. Phys. **B268**, 621 (1986).

[26] B. Grzadkowski, M. Iskrzynski, M. Misiak, and J. Rosiek, J. High Energy Phys. 10 (2010) 085.

[27] X. Zhang and B.-L. Young, Phys. Rev. D **49**, 563 (1994).

[28] D. McKeen, M. Pospelov, and A. Ritz, Phys. Rev. D **86**, 113004 (2012).

[29] A. V. Manohar and M. B. Wise, Phys. Lett. B **636**, 107 (2006).

[30] C. Grojean, E. E. Jenkins, A. V. Manohar, and M. Trotta, J. High Energy Phys. 04 (2013) 016; J. E.-Miró, J. R. Espinosaa, E. Massoa, and A. Pomarol, arXiv:1302.5661.

[31] E. Masso and V. Sanz, Phys. Rev. D **87**, 033001 (2013); P. Agrawal, S. Mitra, and A. Shivaji, arXiv:1211.4362; C. Degrande, N. Greiner, W. Kilian, O. Mattelaer, H. Mebane, T. Stelzer, S. Willenbrock, and C. Zhang, Ann. Phys. (Amsterdam) **335**, 21 (2013); F. Bonnet, M. B. Gavela, T. Ota, and W. Winter, Phys. Rev. D **85**, 035016 (2012); S. Banerjee, S. Mukhopadhyay, and B. Mukhopadhyaya, J. High Energy Phys. 10 (2012) 062; G. Belanger, B. Dumont, U. Ellwanger, J. F. Gunion, and S. Kraml, J. High Energy Phys. 02 (2013) 053; T. Corbett, O. J. P. Eboli, J. Gonzalez-Fraile, and M. C. Gonzalez-Garcia, Phys. Rev. D **87**, 015022 (2013); B. Batell, S. Gori, and L.-T. Wang, J. High Energy Phys. 06 (2012) 172; R. Alonso, M. B. Gavela, L. Merlo, S. Rigolin, and J. Yepes, Phys. Lett. B **722**, 330 (2013); Phys. Rev. D **87**, 055019 (2013).

[32] A. Azatov and J. Galloway, Int. J. Mod. Phys. A **28**, 1330004 (2013); R. Contino, M. Ghezzi, C. Grojean, M. Mühlleitner, and M. Spira, J. High Energy Phys. 07 (2013) 35; J. Ellis and T. You, J. High Energy Phys. 06 (2013) 103; A. Falkowski, F. Riva, and A. Urbano, arXiv:1303.1812; A. Djouadi and G. Moreau, arXiv:1303.6591.

[33] A. V. Manohar and M. B. Wise, Phys. Rev. D **74**, 035009 (2006).

[34] M. E. Peskin and T. Takeuchi, Phys. Rev. D **46**, 381 (1992); Phys. Rev. Lett. **65**, 964 (1990).

[35] J. Erler and P. Langacker "*Electroweak Model and Constraints on New Physics*," http://pdg.lbl.gov/2013/reviews/rpp2012-rev-standard-model.pdf.

[36] A. Djouadi, Phys. Rep. **457**, 1 (2008).

[37] B. L. Ioffe and V. A. Khoze, Fiz. Elem. Chastits At. Yadra **9**, 118 (1978) [Sov. J. Part. Nucl. **9**, 50 (1978)]; M. A. Shifman, A. I. Vainshtein, M. B. Voloshin, and V. I. Zakharov, Yad. Fiz. **30**, 1368 (1979) [Sov. J. Nucl. Phys. **30**, 711 (1979)]; R. Gastmans, S. L. Wu, and T. T. Wu, arXiv:1108.5872; D. Huang, Y. Tang, and Y.-L. Wu, arXiv:1109.4846v2.

[38] J. F. Gunion, H. E. Haber, G. Kane, and S. Dawson, *The Higgs Hunter's Guide* (Westview Press, Boulder, CO, 2000).

[39] L. Bergstrom and G. Hulth, Nucl. Phys. **B259**, 137 (1985); **B276**, 744(E) (1986).

[40] M. Pospelov and A. Ritz, Phys. Rev. D **63**, 073015 (2001); arXiv:hep-ph/0010037v2.

[41] F. Xu, H. An, and X. Ji, J. High Energy Phys. 03 (2010) 088.

[42] W. Dekens and J. de Vries, J. High Energy Phys. 05 (2013) 149.

[43] J. J. Hudson, D. M. Kara, I. J. Smallman, B. E. Sauer, M. R. Tarbutt, and E. A. Hinds, Nature (London) **473**, 493 (2011).

[44] C. A. Baker *et al.*, Phys. Rev. Lett. **97**, 131801 (2006).

[45] I. Bars and M. Yoshimura, Phys. Rev. D **6**, 374 (1972); K. Fujikawa, B. W. Lee, and A. I. Sanda, Phys. Rev. D **6**,

2923 (1972); W. A. Bardeen, R. Gastmans, and B. Lautrup, Nucl. Phys. **B46**, 319 (1972).

[46] G. W. Bennett *et al.* (Muon ($g-2$) Collaboration), Phys. Rev. D **73**, 072003 (2006).

[47] G. F. Giudice, P. Paradisi, and M. Passera, J. High Energy Phys. 11 (2012) 113.

[48] V. Barger, M. Ishida, and W.-Y. Keung, Phys. Rev. Lett. **108**, 261801 (2012).

[49] T. Phehn, M. Spira, and P. M. Zerwas, Nucl. Phys. **B479**, 46 (1996).

[50] X.-G. He, G. Valencia, and H. Yokoya, J. High Energy Phys. 12 (2011) 030; C. P. Burgess, M. Trott, and S. Zuberi, J. High Energy Phys. 09 (2009) 082; L. M. Carpenter and S. Mantry, Phys. Lett. B **703**, 479 (2011); J. Cao, P. Wan, J. M. Yang, and J. Zhu, arXiv:1303.2426.

[51] See, for example, K.-m. Cheung, C.-H. Chou, and O. C. W. Kong, Phys. Rev. D **64**, 111301 (2001); D. Chang, W.-F. Chang, C.-H. Chou, and W.-Y. Keung, Phys. Rev. D **63**, 091301 (2001).

[52] See, for example, T. H. West, Phys. Rev. D **50**, 7025 (1994); T. Kadoyoshi and N. Oshimo, Phys. Rev. D **55**, 1481 (1997); D. Chang, W.-Y. Keung, and A. Pilaftsis, Phys. Rev. Lett. **82**, 900 (1999); **83**, 3972(E) (1999); A. Pilaftsis, Phys. Lett. B **471**, 174 (1999); D. Chang, W.-F. Chang, and W.-Y. Keung, Phys. Lett. B **478**, 239 (2000); Phys. Rev. D **71**, 076006 (2005); G. F. Giudice and A. Romanino, Phys. Lett. B **634**, 307 (2006).

[53] W.-F. Chang and J. N. Ng, J. High Energy Phys. 10 (2005) 091; arXiv:hep-ph/0512334.

[54] T. Plehn, D. L. Rainwater, and D. Zeppenfeld, Phys. Rev. Lett. **88**, 051801 (2002); V. Hankele, G. Klamke, D. Zeppenfeld, and T. Figy, Phys. Rev. D **74**, 095001 (2006); G. Klamke and D. Zeppenfeld, J. High Energy Phys. 04 (2007) 052; F. Campanario, M. Kubocz, and D. Zeppenfeld, Phys. Rev. D **84**, 095025 (2011); C. Englert, M. Spannowsky, and M. Takeuchi, J. High Energy Phys. 06 (2012) 108; S. Berge and W. Bernreuther, Phys. Lett. B **671**, 470 (2009); S. Berge, W. Bernreuther, B. Niepelt, and H. Spiesberger, Phys. Rev. D **84**, 116003 (2011); B. Coleppa, K. Kumar, and H. E. Logan, Phys. Rev. D **86**, 075022 (2012).

[55] K. Hagiwara and M. L. Stong, Z. Phys. C **62**, 99 (1994); M. Kramer, J. H. Kuhn, M. L. Stong, and P. M. Zerwas, Z. Phys. C **64**, 21 (1994); G. J. Gounaris, F. M. Renard, and N. D. Vlachos, Nucl. Phys. **B459**, 51 (1996); S. Y. Choi, K. Hagiwara, and M. S. Baek, Phys. Rev. D **54**, 6703 (1996); G. J. Gounaris and G. P. Tsirigoti, Phys. Rev. D **56**, 3030 (1997); **58**, 059901(E) (1998); E. Gabrielli, V. A. Ilyin, and B. Mele, Phys. Rev. D **60**, 113005 (1999); I. F. Ginzburg, Nucl. Phys. B, Proc. Suppl. **82**, 367 (2000); I. F. Ginzburg and I. P. Ivanov, Eur. Phys. J. C **22**, 411 (2001).

[56] W.-Y. Keung and W. J. Marciano, Phys. Rev. D **30**, 248 (1984).